

LATTICE-REDUCTION AIDED LINEAR EQUALIZATION FOR WIRELESS
COMMUNICATIONS OVER FADING CHANNELS

Except where reference is made to the work of others, the work described in this thesis is my own or was done in collaboration with my advisory committee. This thesis does not include proprietary or classified information.

Wei Zhang

Certificate of Approval:

Jitendra Tugnait
James B. Davis and Alumni Professor
Department of Electrical and Computer
Engineering

Xiaoli Ma, Chair
Assistant Professor
Department of Electrical and Computer
Engineering

Min-Te Sun
Assistant Professor
Department of Computer Science and
Software Engineering

Stephen L. McFarland
Acting Dean
Graduate School

LATTICE-REDUCTION AIDED LINEAR EQUALIZATION FOR WIRELESS
COMMUNICATIONS OVER FADING CHANNELS

Wei Zhang

A Thesis
Submitted to
the Graduate Faculty of
Auburn University
in Partial Fulfillment of the
Requirements for the
Degree of
Master of Science

Auburn, Alabama
May 11, 2006

LATTICE-REDUCTION AIDED LINEAR EQUALIZATION FOR WIRELESS
COMMUNICATIONS OVER FADING CHANNELS

Wei Zhang

Permission is granted to Auburn University to make copies of this thesis at its discretion, upon the request of individuals or institutions and at their expense. The author reserves all publication rights.

Signature of Author

Date of Graduation

VITA

Wei Zhang was born on May 14, 1982 in Qingdao, a beautiful seaside city in China. He graduated from Qingdao No. 2 Middle School in 2000. Then, he attended Zhejiang University in Hangzhou, China. He got his Bachelor of Engineering degree with honors from the Department of Information Science and Electronic Engineering in Chu Kechen Honors College, Zhejiang University in 2004. After that, he joined Auburn University to continue his graduate study in Department of Electrical and Computer Engineering.

THESIS ABSTRACT
LATTICE-REDUCTION AIDED LINEAR EQUALIZATION FOR WIRELESS
COMMUNICATIONS OVER FADING CHANNELS

Wei Zhang

Master of Science, May 11, 2006
(B.S., Zhejiang University, 2004)

73 Typed Pages

Directed by Xiaoli Ma

Modern wireless communications ask for high data rate, high transmission performance and low complexity. High data rate induces frequency-selective channels because of the relatively shorter symbol duration than the delay spread. Wireless links introduce fading which degrades performance and requires diversity techniques to combat. Orthogonal Frequency Division Multiplexing (OFDM) is an effective method to deal with frequency-selective channels since it facilitates low complexity equalization and decoding. To eliminate the effects of the channel nulls and fading, linear precoded OFDM is introduced to enable multipath diversity and the maximum likelihood decoder is used to collect the diversity. But, the low complexity provided by OFDM is sacrificed. Multi-antenna techniques are shown to be able to boost the data rate and also collect space diversity to combat fading. The V-BLAST (Vertical Bell Labs Layered Space-Time) scheme enables higher data rate than single-antenna setup does, but it also requires higher decoding complexity. As a combination, multi-input multi-output (MIMO-) OFDM has been widely studied to boost the transmit-rate and performance

in terms of diversity. For MIMO-OFDM systems, many designs successfully exploit the joint space-multipath diversity when maximum likelihood (ML) detector is adopted at the receiver, which is well known for high complexity. To reduce the decoding complexity, linear equalizers are favored in practical systems, but they usually induce performance degradation. In this thesis, we first quantify the diversity of conventional linear equalizers for linear precoded OFDM, V-BLAST and MIMO-OFDM designs. Then, we propose lattice reduction (LR-) aided equalizers to improve the performance, and show that LR-aided linear equalizers achieve the same diversity order as that collected by ML detectors for (MIMO-) OFDM systems and V-BLAST systems. Simulation results corroborate the theoretical findings.

ACKNOWLEDGMENTS

A journey is easier when you travel together. This thesis is the result of two years of work during which I have been accompanied and supported by many people. It is a pleasure that I now have the opportunity to express my gratitude for them.

First, I would like to express my sincere appreciation to my advisor Dr. Xiaoli Ma for her guidance and support throughout this work. With her enthusiasm and inspiration, this work has been carried out smoothly. During these two years' study, she provided excellent mentoring, but what I benefit most from her is her specially designed training procedure which helped me to transmit from an undergraduate to graduate student successfully. Her persistent encouragement and insightful advice make me believe in my choice which results in this thesis. I owe her lots of gratitude for leading me to the exciting world of wireless communications and showing me the way of performing research. She could not even realize how much I have learned from her. Besides of being an excellent supervisor, Dr. Ma is as close as a good friend to me. I am really glad that I have known Dr. Ma in my life.

I am also grateful for the contributions of Dr. Jitendra Tugnait both as member of my thesis committee and as a great teacher, and for his assistance throughout my graduate studies. My appreciation also goes to Dr. Min-Te Sun from whom I broaden knowledge to computer science from the weekly study group. Also, I thank my colleagues Liying Song and Zhenqi Chen for their helpful discussions and support through this work.

It is not easy to start a new life in a different country. So I will give my appreciation to my friends Wei Feng, Shuangchi He, Jin Li, Tao Li, Weidong Tang and Yuan Yao, with whom my life becomes easier and happier.

I would like to give my special thanks to my dear wife Xiaoming Li for her love and support, and to my parents for their understanding, endless patience and encouragement. As the only child of the family, I owe them a lot for studying abroad.

I would like to acknowledge the financial support provided by the U.S. Army Research Laboratory and the U.S. Army Research Office under grant number W911NF-04-1-0338 and through collaborative participation in the Collaborative Technology Alliance for Communications & Networks sponsored by the U.S. Army Research Laboratory under Cooperative Agreement DAAD19-01-2-0011.

Style manual or journal used Journal of Approximation Theory (together with the style known as “aums”). Bibliography follows van Leunen’s *A Handbook for Scholars*.

Computer software used The document preparation package T_EX (specifically L^AT_EX) together with the departmental style-file aums.sty.

TABLE OF CONTENTS

LIST OF FIGURES	xii
1 INTRODUCTION	1
2 PERFORMANCE ANALYSIS OF LLP-OFDM SYSTEMS	5
2.1 System Model of LLP-OFDM	5
2.2 Linear Equalization For LLP-OFDM	7
2.2.1 ZF Equalizer for LLP-OFDM	8
2.2.2 MMSE Equalizer for LLP-OFDM	12
2.2.3 DFE Equalizer for LLP-OFDM	14
2.3 LR-aided Linear Equalization For LLP-OFDM	15
2.3.1 LR-aided Linear Equalization	16
2.3.2 Performance Analysis on LR-aided Linear Equalizers	18
2.4 Simulation Results	24
3 LINEAR EQUALIZATION FOR V-BLAST SYSTEMS	29
3.1 System Model of V-BLAST Systems	29
3.2 Linear Equalizers and Performance Analysis	30
3.2.1 ZF Equalizers	31
3.2.2 MMSE Equalizers	32
3.3 LR-Aided Linear Equalizers	34
3.4 Simulation Results	35
4 EXTENSION TO MIMO-OFDM SYSTEMS	40
4.1 FDFR-OFDM	40
4.2 STF-OFDM	44
4.3 Simulation Results	47
5 CONCLUDING REMARKS AND FUTURE RESEARCH DIRECTIONS	49
BIBLIOGRAPHY	51
APPENDICES	54
APPENDIX A	55
APPENDIX B	57
APPENDIX C	58

LIST OF FIGURES

2.1	Comparisons among different linear equalizers	24
2.2	Comparisons among different equalizers for LLP-OFDM	25
2.3	Comparisons among different group sizes using ML detector and complex LR-aided equalizer	26
2.4	Complexity comparison of different decoding methods	27
3.1	BER of systems with $N_t = 2$ and $N_r = 2, 3, 4$ separately and BPSK modulation	36
3.2	SER of a system with $(N_t, N_r) = (3, 4)$ and QPSK modulation	37
3.3	Complexity comparison between complex LLL and real LLL algorithms	38
3.4	Performance comparison between the complex and real LLL algorithms with $(N_t, N_r) = (4, 4)$	39
4.1	Block Diagram of MIMO-OFDM	41
4.2	Comparison among different equalizers for FDFR design	47
4.3	Comparison among different equalizers for STF design	48

CHAPTER 1
INTRODUCTION

Modern development of wireless communications requires reliable high-data-rate services. To increase data rate, we can decrease the symbol period, but this will introduce frequency-selectivity (and hence time-dispersive) channels. Orthogonal frequency division multiplexing (OFDM) is known as an effective method to deal with frequency-selective channels since it facilitates low-complexity equalization and decoding [22]. However, the original uncoded OFDM design neither guarantees symbol recovery, nor collects the multipath diversity to combat fading. Several techniques were proposed to collect the multipath diversity provided by the channel. One way to recover the symbol detectability for single antenna OFDM systems, is linear complex-field coded (LCFC-) OFDM (a.k.a. linear precoded OFDM) presented in [11, 22] to collect the multipath diversity but at the cost of increased decoding complexity.

Another way to achieve high-data-rate is to adopt multi-antenna at the transmitter and receiver. Space-time multiplexing of multi-antenna transmissions over multi-input multi-output (MIMO) channels has well documented merits in combating fading, and further enhancing data rates. The V-BLAST (Vertical Bell Labs Layered Space-Time) architecture presented in [4, 25] is a well-known method for achieving high spectral efficiencies over a rich-scattered environment. Since high data rate is achieved through multiple transmit- and receive-antennas, and high order signal constellation is usually used, the high decoding complexity at the receiver for collecting the diversity provided by the channels becomes the bottle-neck of the development of multi-antenna systems.

Frequency-selective MIMO fading channels provide space-multipath diversity to combat fading. Thus, MIMO-OFDM becomes a strong candidate for next generation wireless multi-antenna communications. Numerous space-time (ST) coding schemes have been developed for MIMO-OFDM systems to collect space-multipath diversity (e.g., [11] and [13]). Since all of them used maximum likelihood (ML) detection or near-ML schemes such as sphere-decoding (SD) method, the decoding complexity is high especially when a large number of transmit-antennas and/or high signal constellations are employed. Thus, it is obvious that, no matter in single antenna LCFC-OFDM systems, V-BLAST systems or in MIMO-OFDM systems, how to reduce the decoding complexity while exploiting the diversity order is the problem we would like to study.

The first straightforward thought to solve this problem is to use linear equalizers such as zero-forcing (ZF) and minimum mean square error (MMSE) equalizers. It is well-known that linear detection methods have much lower complexity than ML and SD methods but introducing an inferior performance. Interestingly, it has been shown that even linear equalizers guarantee maximum multipath diversity for *certain* precoded OFDM systems [21] (e.g., the system in [22]). However, the decoding complexity of linear equalizers in [21] depends on the number of subcarriers which usually is large. Grouped LCFC-OFDM design has been proposed in [11] to reduce the decoding complexity by performing smaller size of ML. The major difference for the LCF coder design of [22, 21] and the one in [11] is that LCF coder in [11] depends on the lattice structure of the transmitted symbols. Therefore, to differentiate these two, we call the grouped LCFC-OFDM scheme as linear lattice-based precoded (LLP)-OFDM. In general, the performance of linear equalization has not been studied for LLP-OFDM, V-BLAST and MIMO-OFDM systems in the literature. In this thesis, we analyze the performance

of the linear equalizers for LLP-OFDM systems and extend the results to V-BLAST systems and MIMO-OFDM systems.

Recently LR technique has been used to improve the performance of linear equalizers over MIMO systems (e.g., [8] and [24]). A class of real LR-aided linear equalizers was presented in [26, 27], to transform the system model into an equivalent one with better conditioned channel matrix while maintaining the low complexity. It is shown that LR technique can help to collect the maximum diversity order while does not increase the complexity much. Therefore, in this thesis, we develop complex LR-aided linear equalizers to decode LLP-OFDM systems and analyze the performance in terms of diversity. The results can also be extended to V-BLAST and MIMO-OFDM designs to show the diversity order explicitly.

This thesis is organized as follows. In Chapter 2, we study the performance of LLP-OFDM systems: first, the system model of LLP-OFDM is presented; then the performance of LLP-OFDM systems with three kinds of low-complexity equalizers (ZF, MMSE and decision-feedback equalizer (DFE)) is analyzed separately; LR-aided linear detection methods for LLP-OFDM systems are developed and analyzed. We show that LR-aided linear equalizers exploit multipath diversity. The simulation results will corroborate our theoretical claims. Chapter 3 and Chapter 4 will follow similar structure while Chapter 3 studies the V-BLAST systems and Chapter 4 copes with MIMO-OFDM systems, where two kinds of multi-antenna OFDM designs are analyzed as examples. The last chapter presents concluding remarks and future research directions.

Notation: Upper (lower) bold face letters will be used for matrices (column vectors). Superscript \mathcal{H} denotes Hermitian, $*$ conjugate, and T transpose. We will reserve \otimes for the Kronecker product, $\lceil \cdot \rceil$ for integer ceiling, and $E[\cdot]$ for expectation; $\text{diag}[\mathbf{x}]$ will stand

for a diagonal matrix with \boldsymbol{x} on its main diagonal. \boldsymbol{I}_N will denote the $N \times N$ identity matrix. \mathbb{Z} is the integer set and \mathbb{C} stands for the complex field. $\mathbb{Z}[\sqrt{-1}]$ denotes the Gaussian integer ring whose elements have the form $\mathbb{Z} + \sqrt{-1}\mathbb{Z}$.

CHAPTER 2

PERFORMANCE ANALYSIS OF LLP-OFDM SYSTEMS

In this chapter, we consider single-antenna LLP-OFDM systems. First, the system model of grouped LLP-OFDM is introduced. With this model, the performance of linear equalizers is studied. Then, we develop the complex LR-aided linear equalizers for LLP-OFDM systems and analyze the performance to show it can collect the multi-path diversity.

2.1 System Model of LLP-OFDM

For high-rate transmissions, when the maximum delay spread (τ_d) of the channel exceeds the symbol period (T_s), inter-symbol interference (ISI) cannot be ignored and the channel exhibits frequency-selectivity. Suppose the channel is random, with finite impulse response, consisting of $L + 1$ taps, where L is defined as $\lfloor \tau_d/T_s \rfloor$. Channel taps are denoted as a vector $\mathbf{h} = [h_0, h_1, \dots, h_L]^T$ and modelled as complex Gaussian random variables. Here, the conventional uncoded OFDM system we consider includes cyclic prefix (CP) insertion and inverse FFT (IFFT) operations at the transmitter, and CP removal and FFT operations at the receiver. It has been shown that plain OFDM enables symbol-by-symbol low complexity decoding. However, as stated in [3] and [22], the performance of uncoded OFDM suffers from loss of diversity. LLP-OFDM [11, 12, 22] has been proposed to combat frequency-selective fading by collecting the multipath diversity provided by the channel.

In order to exploit the multipath diversity in OFDM, the LCFC-OFDM designs first linearly encode the i th information block $\mathbf{s}(i) = [s(iN), \dots, s(iN + N - 1)]^T \in \mathbb{Z}[\sqrt{-1}]^{N \times 1}$ (N is much greater than L , but less than the normalized channel coherence time) by a time-invariant matrix $\mathbf{\Gamma} \in \mathbb{C}^{N \times N}$; and then multiplexes the coded symbols $\mathbf{u}(i) = \mathbf{\Gamma}\mathbf{s}(i) \in \mathbb{C}^{N \times 1}$ using conventional OFDM. Collecting the i th received OFDM block after CP removal and FFT operations as: $\mathbf{y}(i) = [y(iN), \dots, y(iN + N - 1)]^T$, the input-output (I/O) relationship of the overall system model can be expressed as:

$$\mathbf{y}(i) = \mathbf{D}_H \mathbf{u}(i) + \mathbf{w}(i) = \mathbf{D}_H \mathbf{\Gamma} \mathbf{s}(i) + \mathbf{w}(i), \quad (2.1)$$

where $\mathbf{D}_H = \text{diag}[H(0), H(1), \dots, H(N - 1)]$, with $H(n) = \sum_{l=0}^L h_l e^{-j2\pi ln/N}$. $\mathbf{w}(i)$ is the i th white complex Gaussian noise vector observed at the receiver with zero mean and covariance matrix $\sigma_w^2 \mathbf{I}_N$. Since we consider block-by-block decoding, for notational simplicity, we will drop our OFDM block index i from now on.

There are several ways to design $\mathbf{\Gamma}$ to achieve maximum diversity without any channel knowledge at the transmitter. One way is to design $\mathbf{\Gamma}$ as a tall Vandermonde matrix with properly chosen generators [22]. For this case, though the bandwidth efficiency is sacrificed, it has been proved that even linear equalizers (ZF and MMSE) can also achieve the full diversity [21]. But since the complexity of linear equalizers in [21, 22] depends on the block size N with a order of $\mathcal{O}(N^3)$, when N is large, even linear equalizers require high decoding complexity.

Another way to design the LCF encoder uses algebraic number theory and grouping method [11]. Suppose the N subcarriers are split into N_g groups and each group has size K . To achieve the maximum coding gain, we select the g th group as [11] and [12]:

$\mathbf{s}_g = [s(g), s(g + N_g), \dots, s(g + (K - 1)N_g)]^T$, with $s(n)$ denoting the n th symbol in \mathbf{s} . The K equi-spaced symbols are precoded (or linear block coded) by a $K \times K$ unitary matrix Θ , and the precoded symbol $\mathbf{u}_g = \Theta \mathbf{s}_g$ is mapped into K equi-spaced carriers. It is readily seen that analogous to (2.1), the I/O relationship for the g th group becomes:

$$\mathbf{y}_g = \mathbf{D}_{H,g} \Theta \mathbf{s}_g + \mathbf{w}_g = \mathbf{H}_{equ} \mathbf{s}_g + \mathbf{w}_g, \quad (2.2)$$

where $\mathbf{H}_{equ} := \mathbf{D}_{H,g} \Theta$ is the equivalent channel matrix with $\mathbf{D}_{H,g} = \text{diag}[H(g), H(g + N_g), \dots, H(g + (K - 1)N_g)]$, and \mathbf{w}_g is the corresponding noise of the g th group. We observe that the I/O relationship of the g th group in (2.2) has the same form as (2.1). Thus, ML or SD method can be used to collect full multipath diversity. As proposed in [12, 11], the maximum achievable multipath diversity order is $G_d = \min(K, R_h)$, where R_h denotes the rank of the channel coefficients correlation matrix $E(\mathbf{h}\mathbf{h}^H)$.

Compared with the ungrouped version in [22], grouped LLP-OFDM has lower complexity since each group only has $K < N$ symbols. However, ML or near-ML decoder is required to collect multipath diversity. One natural question now is what if one wants to further reduce the complexity and just uses linear equalizer to (2.2) and what the diversity is in this case. In the next section, we analyze the performance of the linear equalizers for LLP-OFDM systems and answer this question. For brevity, we will drop the group index g in (2.2).

2.2 Linear Equalization For LLP-OFDM

Linear equalizers are favored in practical systems because they have the lowest complexity among all kinds of detection methods. However, at the same time, linear

equalizers are “blamed” because they usually have inferior and unpredicted performance (e.g., unknown diversity order). In the literature, the performance in terms of diversity with optimal decoders (e.g., ML) has been well-documented (see e.g., [18, 12]). However, the performance of linear equalizers is not well studied. Recently, it has been shown that even linear equalizers can collect the multipath diversity for LLP-OFDM with tall Vandermonde LCF encoders [21], while it is unclear on the performance of LLP-OFDM with linear equalizers. In this section, we study the performance of LLP-OFDM systems with ZF equalizer, MMSE equalizer and decision-feedback equalizer (DFE). We will keep our proofs general so that they can be applied to other linear systems.

2.2.1 ZF Equalizer for LLP-OFDM

Suppose that the receiver has perfect channel knowledge. Based on the model in (2.2), the output of ZF equalizer is given as:

$$\mathbf{x} = (\mathbf{H}_{equ})^{-1} \mathbf{y} = \mathbf{s} + (\mathbf{H}_{equ})^{-1} \mathbf{w} = \mathbf{s} + \mathbf{n}, \quad (2.3)$$

where $\mathbf{n} := \mathbf{H}_{equ}^{-1} \mathbf{w}$ is the noise after equalization. The channel matrix $\mathbf{H}_{equ} = \mathbf{D}_H \mathbf{\Theta}$ has full rank with probability one (wp1) because $\mathbf{\Theta}$ is a unitary matrix and the diagonal matrix \mathbf{D}_H has full rank wp1. Note that the noise vector \mathbf{n} is no longer white and its covariance matrix depends on the equalization matrix \mathbf{H}_{equ}^{-1} . The next step is to map the output to signal constellation:

$$\hat{s}_i = \mathcal{Q}(x_i) = \arg \min_{s \in \mathcal{S}} |x_i - s|, \quad (2.4)$$

where x_i denotes the i th element of \mathbf{x} and $\mathcal{Q}(\cdot)$ means the quantization of the symbol.

Starting from (2.3), we now analyze the diversity collected by ZF equalizer. Suppose that the i th transmitted symbol is s_i , and at the receiver it is erroneously decoded as $\tilde{s}_i \neq s_i$. The error probability is given as:

$$P(s_i \rightarrow \tilde{s}_i | \mathbf{H}_{equ}) = P(|x_i - \tilde{s}_i|^2 < |x_i - s_i|^2 | \mathbf{H}_{equ}),$$

where n_i is the i th element of \mathbf{n} . If we define $e_i = s_i - \tilde{s}_i$, then the error probability can be further simplified as:

$$\begin{aligned} P(s_i \rightarrow \tilde{s}_i | \mathbf{H}_{equ}) &= P(|e_i + n_i|^2 < |n_i|^2 | \mathbf{H}_{equ}) \\ &= P\left(\frac{-e_i n_i^* - e_i^* n_i}{2} > \frac{|e_i|^2}{2} \middle| \mathbf{H}_{equ}\right). \end{aligned} \quad (2.5)$$

Though as we stated, the ZF equalized noise vector \mathbf{n} is no longer white, it is not difficult to verify that for each channel realization, \mathbf{n} is still complex Gaussian distributed with zero mean and covariance matrix

$$E[\mathbf{n}\mathbf{n}^H] = \sigma_w^2 (\mathbf{H}_{equ}^H \mathbf{H}_{equ})^{-1} = \sigma_w^2 \mathbf{C}, \quad (2.6)$$

where $\mathbf{C} := (\mathbf{H}_{equ}^H \mathbf{H}_{equ})^{-1}$. Define a random variable $v_i = (-e_i n_i^* - e_i^* n_i)/2$. Given the error symbol e_i , v_i is real Gaussian distributed with zero mean and variance $|e_i|^2 E[|n_i|^2]/2 = |e_i|^2 \sigma_w^2 C_{ii}/2$, where C_{ii} is the (i, i) th element of \mathbf{C} in (2.6). Thus, the error probability in (2.5) can be re-written as:

$$P(s_i \rightarrow \tilde{s}_i | \mathbf{H}_{equ}) = Q\left(\sqrt{\frac{|e_i|^2}{2\sigma_w^2 C_{ii}}}\right). \quad (2.7)$$

Based on (2.7), the diversity order collected by the ZF equalizer is established in the following:

Proposition 1 *Given the model in (2.2), if the channel taps are complex Gaussian distributed with zero mean, then the ZF equalizer in (2.3) exists wp1 and collects diversity order 1 over LLP-OFDM systems with frequency-selective channels.*

Proof: According to the design in [11] or [12], there exists at least one unitary matrix Θ that enables maximum diversity for any block size K and constellations that belong to Gaussian integer ring. The diagonal matrix \mathbf{D}_H has full rank wp1. Thus, both of them are invertible wp1. This shows the ZF equalizer exists wp1.

Because Θ is unitary and recalling the Vandermonde structure of Θ , we notice that the elements of Θ have amplitude $1/\sqrt{K}$. Thus, matrix \mathbf{C} in (2.6) can be written as

$$\mathbf{C} = (\mathbf{H}_{equ}^{\mathcal{H}} \mathbf{H}_{equ})^{-1} = (\Theta^{\mathcal{H}} \mathbf{D}_H^{\mathcal{H}} \mathbf{D}_H \Theta)^{-1} = \Theta^{\mathcal{H}} \mathbf{D}_H^{-1} (\mathbf{D}_H^{\mathcal{H}})^{-1} \Theta,$$

and the (i, i) th entry of \mathbf{C} , C_{ii} becomes

$$C_{ii} = \boldsymbol{\theta}_i^{\mathcal{H}} \mathbf{D}_H^{-1} (\mathbf{D}_H^{\mathcal{H}})^{-1} \boldsymbol{\theta}_i = \frac{1}{K} \sum_{k=0}^{K-1} \frac{1}{|H(k)|^2} \quad (2.8)$$

where $\boldsymbol{\theta}_i$ is the i th column of the LCF encoder Θ . Based on (2.8), we can bound C_{ii} as :

$$\frac{1}{K |H(c)|^2} \leq C_{ii} \leq \frac{1}{\min_{0 \leq k \leq K-1} |H(k)|^2} \quad (2.9)$$

where c is any integer, $c \in [0, K - 1]$. The left inequality holds because C_{ii} is the summation of K nonnegative numbers and is surely larger than or equal to any one of

them. The right inequality holds because $\frac{1}{|H(k)|^2} \leq \frac{1}{\min_{0 \leq i \leq K-1} |H(i)|^2}$ for any $0 \leq k \leq K-1$. According to (2.7), the post-processing signal-to-noise ratio (SNR) of ZF equalizer is $\gamma = \frac{|e_i|^2}{2\sigma_w^2 C_{ii}}$. Plugging the inequality (2.9) into (2.7), we will have:

$$\frac{K|e_i|^2|H(c)|^2}{2\sigma_w^2} \geq \gamma = \frac{|e_i|^2}{2\sigma_w^2 C_{ii}} \geq \frac{|e_i|^2 \min_{0 \leq k \leq K-1} |H(k)|^2}{2\sigma_w^2}. \quad (2.10)$$

Thus, the outage probability [23] can be bounded as:

$$P\left(|H(c)|^2 \leq \frac{2\sigma_w^2 \gamma^{th}}{K|e_i|^2}\right) \leq P(\gamma < \gamma^{th}) \leq P\left(\min_{0 \leq k \leq K-1} |H(k)|^2 \leq \frac{2\sigma_w^2 \gamma^{th}}{|e_i|^2}\right). \quad (2.11)$$

Next, to show the diversity order collected by ZF equalizer, we need the following lemma:

Lemma 1 *Given N random variables X_1, X_2, \dots, X_N (either dependent or independent), they are all central Chi-square distributed with degrees of freedom $2M$. Let X_{min} denote the minimum of them, and then we have $P(x_{min} < \epsilon) \leq c_u \epsilon^M$, where c_u is a constant depending on N and M .*

The proof is given in Appendix A. Since $|H(k)|^2$ is exponentially distributed (or Chi-square distributed with degrees of freedom 2), according to Lemma 1, we can obtain:

$$P\left(\min_{0 \leq k \leq K-1} |H(k)|^2 \leq \frac{2\sigma_w^2 \gamma^{th}}{|e_i|^2}\right) \leq c_u \gamma^{th} \left(\frac{|e_i|^2}{2\sigma_w^2}\right)^{-1}$$

So the performance upper-bound in (2.11) shows diversity one. Since $H(c)$ is complex Gaussian distributed, $|H(c)|^2$ is Chi-square distributed with degrees of freedom 2. Then,

we can obtain that:

$$P\left(|H(c)|^2 \leq \frac{2\sigma_w^2\gamma^{th}}{K|e_i|^2}\right) = \exp\left(-\frac{\sigma_w^2\gamma^{th}}{K|e_i|^2}\right),$$

which shows that the performance lower-bound also has diversity one (see also [23] for similar argument).

So the diversity order of the outage probability is just 1. According to [23], the diversity of outage probability is the same as that of average error probability. Thus, the diversity collected by the ZF equalizer for LLP-OFDM system is just 1. ■

Interestingly, different from the claim in [21], Proposition 1 shows that if we use ZF linear equalizer for LLP-OFDM systems, the diversity order for the performance is only 1. This is because of the different structures of the precoders in [11, 22]. For LLP-OFDM, although the ZF equalizer has low complexity, it cannot collect any multipath diversity.

2.2.2 MMSE Equalizer for LLP-OFDM

Another often used linear equalizer is minimum mean square error (MMSE) equalizer. Based on the model in (2.2), the linear MMSE equalizer for LLP-OFDM systems is given as:

$$\mathbf{x} = (\mathbf{H}_{equ}^H \mathbf{H}_{equ} + \sigma_w^2 \mathbf{I}_K)^{-1} \mathbf{H}_{equ}^H \mathbf{y}. \quad (2.12)$$

It is easy to verify that the MSE of the symbols after MMSE equalization is

$$E[\|\mathbf{s} - \hat{\mathbf{s}}\|^2] = \sigma_w^2 (\mathbf{H}_{equ}^H \mathbf{H}_{equ} + \sigma_w^2 \mathbf{I}_K)^{-1}. \quad (2.13)$$

Defining $\mathbf{C} = (\mathbf{H}_{equ}^H \mathbf{H}_{equ} + \sigma_w^2 \mathbf{I}_K)^{-1}$ and plugging in the fact that $\mathbf{H}_{equ} = \mathbf{D}_H \boldsymbol{\Theta}$ into \mathbf{C} , we have the (i, i) th entry of \mathbf{C}

$$C_{ii} = \boldsymbol{\theta}_i^H (\mathbf{D}_H^H \mathbf{D}_H + \sigma_w^2 \mathbf{I}_K)^{-1} \boldsymbol{\theta}_i = \frac{1}{K} \sum_{k=1}^K \frac{1}{|H(k)|^2 + \sigma_w^2}. \quad (2.14)$$

The approximate BER after MMSE equalization is [16]:

$$P_e \approx \sum_m \alpha_m Q \left(\beta_m \sqrt{\frac{1}{\sigma_w^2 C_{ii}} - 1} \right), \quad (2.15)$$

where α_m and β_m depend on the symbol constellation. Based on (2.14), we find that the SNR for the error probability is bounded by:

$$\frac{\min_{0 \leq k \leq K-1} |H(k)|^2}{\sigma_w^2} \leq \frac{1}{\sigma_w^2 C_{ii}} - 1 \leq \frac{K}{\sigma_w^2} (|H(c)|^2 + \sigma_w^2). \quad (2.16)$$

Similar to the ZF equalizer case, based on (2.16), the diversity order collected by the MMSE equalizer is established in the following:

Proposition 2 *Given the model in (2.2), if the channel taps are complex Gaussian distributed with zero mean, then the MMSE equalizer in (2.12) for the LLP-OFDM system collects diversity order 1.*

2.2.3 DFE Equalizer for LLP-OFDM

Generalized decision feedback equalizer (GDFE) is proposed and compared with the Nulling-Cancelling (NC) equalization ([6]) in [5]. It is shown that the operation of GDFE is equivalent to the NC processing. There are two types of GDFE: ZF-GDFE and MMSE-GDFE. Here, we consider the performance of ZF-GDFE while it is straightforward to see the performance of MMSE-GDFE following the similar analysis. For ZF-GDFE (or ZF-NC), the output of the forward equalizer is:

$$\mathbf{x} = \mathbf{Q}^H \mathbf{y}, \quad (2.17)$$

where \mathbf{QR} is the QR-decomposition of \mathbf{H}_{equ} with unitary matrix \mathbf{Q} and upper triangular matrix \mathbf{R} . Then the decision process becomes

for $n = 0 : K - 1$

$$\hat{s}_{K-n} = \mathcal{Q}((x_{K-n} - \sum_{i=1}^p R_{K-n, K-n+i} \hat{s}_{K-n+i}) / R_{K-n, K-n})$$

end

where $\mathbf{R}_{p,q}$ is the (p, q) th entry of \mathbf{R} and x_i is the i th entry of \mathbf{x} . According to [5], the diversity of LLP-OFDM systems with ZF-GDFE equalizer is determined by the lowest degrees of freedom of $|R_{k,k}|^2, k \in [1, K]$, where \mathbf{R} is the QR decomposition of $\mathbf{D}_H \Theta$ and $R_{k,k}$ is the (k, k) th entry of \mathbf{R} . Considering the QR decomposition process, $R_{K,K}$ offers the lowest degrees of freedom. Because $\mathbf{C} = (\mathbf{H}_{equ}^H \mathbf{H}_{equ})^{-1} = (\mathbf{R}^H \mathbf{R})^{-1}$, it can be verified that $|R_{K,K}|^2 = C_{KK}^{-1}$ satisfies:

$$\min_{0 \leq k \leq K-1} |H(k)|^2 \leq |R_{KK}|^2 \leq K |H(c)|^2. \quad (2.18)$$

Thus, following the analysis for ZF equalizer, we can see that the maximum diversity order that ZF-GDFE can collect is just 1. Similarly, the diversity of the LLP-OFDM systems with MMSE-GDFE is also 1. Proof is omitted here.

Remark 1 From our analysis, we notice that for LLP-OFDM systems, the linear equalizers cannot exploit any multipath diversity, though they have much lower decoding complexity compared with ML or SD methods. Furthermore, the performance of ZF equalizer is the worst among these three linear equalizers while MMSE-GDFE equalizer has the best performance of them.

2.3 LR-aided Linear Equalization For LLP-OFDM

As we know, for linear systems, if \mathbf{H}_{equ} in (2.2) is diagonal, ZF equalizer has the same performance as ML decoder (e.g., for plan OFDM case). However, in general \mathbf{H}_{equ} is not diagonal, and thus ZF equalizer has inferior performance (e.g., in Section III we have shown that ZF equalizer cannot collect multipath diversity). This motivates us to find a way to make \mathbf{H}_{equ} close to a diagonal matrix.

If the symbols \mathbf{s} are drawn from Gaussian integer ring (QAM, PAM constellations), then $\mathbf{H}_{equ}\mathbf{s}$ belongs to a lattice generated by the columns of \mathbf{H}_{equ} . Thus, to estimate the information symbols is equivalent to searching for the closet point in the lattice [1]. The motivation to use lattice reduction (LR) technique in equalization is to make the decision region of the linear equalizers more like that of ML detector by finding a more orthogonal basis for the lattice, thus increase the performance. Recently, Lenstra-Lenstra-Lovász (LLL) algorithm has been adopted for LR-aided linear equalizers to find more orthogonal basis for communication MIMO channels, because it guarantees polynomial complexity

to find a set of bases within a factor of the shortest vectors (see e.g., [8, 24, 27]). The LLL reduction was first posted in [10]. The LR-aided linear equalizers were first applied to MIMO systems (see e.g., [8, 24, 27]). However, the methods in [24, 26, 27] are based on real lattice reduction methods, which increase the decoding complexity by splitting the complex channels into real and imaginary parts. [8] uses complex lattice reduction method, but only for two-transmit-antenna case. In [14], it is mentioned that complex LLL algorithm can be extended to any number of transmit-antennas. Unfortunately, detailed complex LLL algorithm is not provided in [14]. In general, these existing results show that LR performed on the channel matrix can improve the linear detectors' performance while does not increase the complexity much.

2.3.1 LR-aided Linear Equalization

We first extend the LLL algorithm to complex field for any number of transmit-antenna. Our proposed complex LLL algorithm can be found in Appendix B, where we use the conventional MATLAB notation (e.g., $\mathbf{R}(k, k)$ denotes the (k, k) th element of matrix \mathbf{R}). Compared with the real LLL algorithm in [27], the major difference of the complex LLL algorithm exists at Steps (8) and (16) in Table 1. Later by simulations, we show that the complex LLL algorithm enables lower computational complexity than the real LLL algorithm without sacrificing any performance.

Given the system model in (2.2), we adopt CLLL algorithm to reduce the lattice basis of \mathbf{H}_{equ} and obtain $\tilde{\mathbf{H}} = \mathbf{H}_{equ}\mathbf{T}$, where \mathbf{T} is a unimodular matrix which means all the entries of \mathbf{T} and \mathbf{T}^{-1} are Gaussian integers and the determinant of \mathbf{T} is ± 1 or $\pm j$. Then, we apply the LR-aided ZF equalizer $\tilde{\mathbf{H}}^{-1}$ instead of \mathbf{H}_{equ}^{-1} , and the output can be

S1: Map the information bits to symbols s whose constellation belongs to Gaussian integer ring;
S2: Obtain (2.2) after LLP-OFDM transceiver operations;
S3: Perform the Complex LLL algorithm to reduce the lattice basis of the equivalent channel matrix: $[\tilde{\mathbf{H}}, \mathbf{T}] = CLLL(\mathbf{H}_{equ})$;
S4: Rewrite the system as $\mathbf{y} = \mathbf{H}_{equ}\mathbf{T}(\mathbf{T}^{-1}\mathbf{s}) + \mathbf{w} = \tilde{\mathbf{H}}\mathbf{z} + \mathbf{w}$;
S5: Apply the ZF equalization based on the new system to obtain $\hat{\mathbf{z}} = \mathcal{Q}(\tilde{\mathbf{H}}^{-1}\mathbf{y})$;
S6: Use $\hat{\mathbf{z}}$ and \mathbf{T} to recover the original information: $\hat{\mathbf{s}} = \mathcal{Q}(\mathbf{T}\hat{\mathbf{z}})$.

Table 2.1: Lattice-Reduction Aided ZF Equalization

written as [c.f. (2.2)]:

$$\mathbf{x} = \mathbf{T}^{-1}\mathbf{s} + \tilde{\mathbf{H}}^{-1}\mathbf{w} = \mathbf{z} + \mathbf{n}. \quad (2.19)$$

Since all the entries of \mathbf{T}^{-1} and the signal constellation belong to Gaussian integer ring, the entries of \mathbf{z} are also Gaussian integers. One can estimate \mathbf{z} from \mathbf{x} by quantization. After obtaining \mathbf{z} , one can recover \mathbf{s} by using \mathbf{T} and mapping to the appropriate constellation. We summarize the main steps of LR-aided ZF equalizer for LLP-OFDM systems in Table .

Note that the equivalent channel matrix \mathbf{H}_{equ} can be other communication channels (e.g. MIMO channel matrix later in Chapter 3, MIMO-OFDM matrices in Chapter 4). To perform the LR-aided MMSE equalizer, we cannot just apply the conventional MMSE equalizer to the new system in Step **S4**, because the average power of \mathbf{z} is not easy to determine. In [27], it shows that LR-aided MMSE equalizer agrees to the LR-aided ZF equalizer with respect to an extended system. Compared with the conventional linear equalizers, LR-aided linear equalizers increase the complexity only in the CLLL reduction step, we will compare the complexity over different systems by simulations.

Remark 2 Here, we notice that in Step **S5**, the quantization of $\tilde{\mathbf{H}}^{-1}\mathbf{y}$ is simply rounding to the nearest integer in order to reduce the complexity. Thus, we must make sure the constellation of symbols s belongs to Gaussian integer ring, and both the real and the imaginary parts are drawn from an integer set whose elements are consecutive integers, or can be transferred to consecutive integers by shifting and scaling. Otherwise, for each realization of channel \mathbf{H}_{equ} , one needs to calculate \mathbf{T} and then find the set of possible $\hat{\mathbf{z}}$. Typically, M -QAM constellations satisfy this prerequisite, e.g., 4-QAM symbols s whose constellation is $\{\pm 1 \pm j\}$, can be transferred to $\{1(0)+1(0)j\}$ by performing $\frac{1}{2}(s+1+j)$. Different from the simple rounding in Step **S5**, the quantization in Step **S6** is to map the product of \mathbf{T} and $\hat{\mathbf{z}}$ to the original information constellation.

2.3.2 Performance Analysis on LR-aided Linear Equalizers

In this section, we prove the diversity order collected by LR-aided linear equalizers. To make our proof compact, we introduce some important definition and lemmas first.

Definition 1 An orthogonality deficiency (*od*) of an $M \times N$ matrix $\mathbf{B} = [\mathbf{b}_1, \mathbf{b}_2, \dots, \mathbf{b}_N]$ as:

$$od(\mathbf{B}) = 1 - \frac{\det(\mathbf{B}^T \mathbf{B})}{\prod_{n=1}^N |\mathbf{b}_n|^2} \quad (2.20)$$

where $|\mathbf{b}_n|, 1 \leq n \leq N$ is the norm of the n th column of \mathbf{B} .

Note that $0 \leq od(\mathbf{B}) \leq 1, \forall \mathbf{B}$ and if \mathbf{B} is singular, $od(\mathbf{B}) = 1$; and if the columns of \mathbf{B} are orthogonal, $od(\mathbf{B}) = 0$. It has been shown that LLL algorithm tries to reduce the

od of the studied matrix [10]. The quantitative result on od reduction is given in the following lemma:

Lemma 2 *Given a matrix $\mathbf{H} \in \mathbb{C}^{M \times N}$ with rank N , $\tilde{\mathbf{H}}$ is obtained after applying complex LLL (CLLL) algorithm with parameter δ on \mathbf{H} [30]. Then, the orthogonality deficiency of $\tilde{\mathbf{H}}$ satisfies:*

$$\sqrt{1 - od(\tilde{\mathbf{H}})} \geq \left(\frac{4}{4\delta - 1} \right)^{-N(N-1)/4} := c_\delta, \quad (2.21)$$

where c_δ is determined by δ and N , and δ can be any fixed real number in $(1/4, 1)$.

For real \mathbf{H} , Lemma 2 is consistent with the result in [10, Proposition 1.8]. Here, we extend it to complex field according to the CLLL algorithm in [30]. Given δ and any integer $N \geq 1$, c_δ is always less than 1. Therefore, the $od(\mathbf{H})$ is bounded by $1 - c_\delta^2$. If \mathbf{H} is singular, i.e., $\text{rank}(\mathbf{H}) < N$, then Lemma 2 does not hold true. In this case, we need to reduce the size of \mathbf{H} and then apply CLLL algorithm.

Since information symbols \mathbf{s} belong to Gaussian integer ring, then $\mathbf{H}\mathbf{s}$ generates a lattice $\mathbf{L} \in \mathbb{C}^{M \times 1}$ with a set of basis vectors $\mathbf{H} = [\mathbf{h}_1, \mathbf{h}_2, \dots, \mathbf{h}_N]$. The following lemma shows an important statistical property of the minimum distance of the lattice \mathbf{L} , which will be useful for our proof on diversity order.

Lemma 3 *Let $\mathbf{H} = [\mathbf{h}_1, \mathbf{h}_2, \dots, \mathbf{h}_N]$ be a set of bases for a lattice \mathbf{L} in $\mathbb{C}^{M \times 1}$. Define \mathbf{h}_{min} as the vector in \mathbf{L} which has the minimum non-zero norm among all the vectors. If all entries of \mathbf{H} are complex Gaussian distributed with zero mean, the following inequality*

holds:

$$P\{|\mathbf{h}_{min}|^2 \leq \epsilon\} \leq c_h \epsilon^D, \quad (2.22)$$

where c_h is a constant determined by N and M , and

$$D = \min_{\forall \mathbf{p} \neq \mathbf{0}} \text{rank}(E(\mathbf{p}\mathbf{p}^H)), \quad (2.23)$$

where $\mathbf{p} \in \mathbf{L}$ and $\mathbf{p} \neq \mathbf{0}$.

The proof can be found in Appendix C. From Lemma 3 we notice that the degrees of freedom D of \mathbf{h}_{min} is determined by the minimum rank of all possible covariance matrices generated by the vectors \mathbf{L} . Apparently, it depends on the covariance matrices of each column \mathbf{h}_n and the cross-correlation among the columns.

To facilitate the use of Lemma 3, we give a corollary as follows:

Corollary 1 *Let $\mathbf{H} = [\mathbf{h}_1, \mathbf{h}_2, \dots, \mathbf{h}_N]$ be a set of bases for a lattice \mathbf{L} in $\mathbb{C}^{M \times 1}$. If 1) all the entries of \mathbf{H} are complex Gaussian distributed with zero mean; 2) $\text{rank}(E[\mathbf{h}_n \mathbf{h}_n^H]) = D, \forall n \in [1, N]$; and 3) all the columns are linear independent with each other on the Gaussian integer ring, then we have $P\{|\mathbf{h}_{min}|^2 \leq \epsilon\} \leq c_h \epsilon^D$.*

Now we are ready to analyze the diversity order collected by the LR-aided ZF equalizer for the LLP-OFDM systems which is quantified in the following proposition:

Proposition 3 *Considering an LLP-OFDM system with group size of K and frequency-selective channel order of L , given the model in (2.2), the diversity order collected by an*

LR-aided ZF equalizer is $\min(K, R_h)$ which is the same as that obtained by ML detector, where $R_h = E[\mathbf{h}\mathbf{h}^T]$ and $\mathbf{h} = [h(0), \dots, h(L)]^T$.

Proof: The output of the LR-aided ZF equalizer is stated in (2.19). Because the entries of \mathbf{z} are integers, if the real and imaginary parts of each entry of $\mathbf{n} = \tilde{\mathbf{H}}^{-1}\mathbf{w}$ are in the interval $(-\frac{1}{2}, \frac{1}{2})$, one is able to decode \mathbf{z} correctly and thus obtain \mathbf{s} correctly. Let us denote $\tilde{\mathbf{H}}^{-1}$ as $[\mathbf{a}_0, \mathbf{a}_1, \dots, \mathbf{a}_{K-1}]^T$, where $\mathbf{a}_i^T, i \in [0, K-1]$ is the i th row of $\tilde{\mathbf{H}}^{-1}$. Hence, if $|\mathbf{a}_i^T\mathbf{w}|$ is less than $\frac{1}{2}$, we will definitely decode the i th symbol correctly. Thus, $P_{e|H_{equ}}$, the error probability for a given \mathbf{H}_{equ} is upper-bounded by

$$P_{e|H_{equ}} \leq P\left(|\mathbf{a}_i^T\mathbf{w}| \geq \frac{1}{2} \middle| \mathbf{H}_{equ}\right).$$

From [19, Lemma 1], we obtain the following inequality:

$$|\mathbf{a}_i^T| \leq \frac{1}{\sqrt{1 - od(\tilde{\mathbf{H}})|\tilde{\mathbf{h}}_i|}} \quad (2.24)$$

where $\tilde{\mathbf{h}}_i, i \in [0, K-1]$ represents the i th column of $\tilde{\mathbf{H}}$. Because

$$|\mathbf{a}_i^T\mathbf{w}| \leq |\mathbf{a}_i^T||\mathbf{w}| \leq \frac{|\mathbf{w}|}{\sqrt{1 - od(\tilde{\mathbf{H}})|\tilde{\mathbf{h}}_i|}},$$

if $|\mathbf{w}|$ is less than $\frac{1}{2}\sqrt{1 - od(\tilde{\mathbf{H}})|\tilde{\mathbf{h}}_i|}$, we will have $|\mathbf{a}_i^T\mathbf{w}| \leq \frac{1}{2}$. Furthermore, since $\tilde{\mathbf{H}}$ is reduced from \mathbf{H}_{equ} using CLLL algorithm, $\sqrt{1 - od(\tilde{\mathbf{H}})} \leq (\frac{4}{4\delta-1})^{-K(K-1)/4}$ according to Lemma 2 wp1. Define $\mathbf{H}_{equ} := [\mathbf{h}_0, \mathbf{h}_1, \dots, \mathbf{h}_{K-1}]$, where $\mathbf{h}_i, i \in [0, K-1]$ is the i th column of \mathbf{H}_{equ} . Let \mathbf{h}_{min} represent the vector with minimum non-zero norm of all the vectors in the lattice generated by \mathbf{H}_{equ} . Since \mathbf{T} is unimodular, $\tilde{\mathbf{H}}$ spans the same

lattice as \mathbf{H}_{equ} . It is easy to verify that $|\mathbf{h}_{min}|$ is less than or equal to $\min_{1 \leq i \leq K} |\tilde{\mathbf{h}}_i|$. Thus, we can see that if $|\mathbf{w}|$ is less than $\frac{1}{2}c_\delta|\mathbf{h}_{min}|$, then $|\mathbf{w}|$ is less than $\frac{1}{2}\sqrt{1 - od(\tilde{\mathbf{H}})}|\tilde{\mathbf{h}}_i|$ for any $i \in [1, K]$. Here we notice that though c_δ is independent on \mathbf{H}_{equ} , \mathbf{h}_{min} depends on \mathbf{H}_{equ} . In summary, we have:

$$P_{e|\mathbf{H}_{equ}} \leq P\left(|\mathbf{a}_i^T \mathbf{w}| \geq \frac{1}{2} \middle| \mathbf{H}_{equ}\right) \leq P\left(|\mathbf{w}| \geq \frac{1}{2}c_\delta|\mathbf{h}_{min}| \middle| \mathbf{H}_{equ}\right). \quad (2.25)$$

Since \mathbf{w} is complex Gaussian white noise, $|\mathbf{w}|^2$ is a central Chi-square random variable with degrees of freedom $2K$ and mean $K\sigma_w^2$. Thus, by averaging (2.25) with respect to the random matrix \mathbf{H}_{equ} (or \mathbf{h}_{min} , the error probability can be further simplified as:

$$\begin{aligned} P_e &\leq E_H \left[P\left(|\mathbf{w}| \geq \frac{1}{2}c_\delta|\mathbf{h}_{min}| \middle| \mathbf{H}_{equ}\right) \right] \\ &\leq P\{(c_\delta|\mathbf{h}_{min}|)^2 \leq 4K\sigma_w^2\} P\{|\mathbf{w}|^2 \geq K\sigma_w^2\} \\ &\quad + P\{4K\sigma_w^2 \leq (c_\delta|\mathbf{h}_{min}|)^2 \leq 4t^2K\sigma_w^2\} P\{|\mathbf{w}|^2 \geq t^2K\sigma_w^2\} \\ &\quad + P\{4t^2K\sigma_w^2 \leq (c_\delta|\mathbf{h}_{min}|)^2 \leq 4t^3K\sigma_w^2\} P\{|\mathbf{w}|^2 \geq t^3K\sigma_w^2\} + \dots \end{aligned} \quad (2.26)$$

where t is a positive constant that satisfies $t > 1$. Here, we notice that all the entries of \mathbf{H}_{equ} are complex Gaussian distributed with zero mean and all the columns are linear independent with each other with probability one. Furthermore, the rank of the covariance matrices of $\mathbf{h}_i, i \in [0, K-1]$ is $\min(K, R_h)$ [11]. With these three conditions satisfied, according to Corollary 1, we have $P\{|\mathbf{h}_{min}|^2 \leq \epsilon\} \leq c_h \epsilon^{\min(K, R_h)}$. Thus, we can get the probability that:

$$P\{(c_\delta|\mathbf{h}_{min}|)^2 \leq aK\sigma_w^2\} \leq c_h \cdot \left(\frac{aK\sigma_w^2}{c_\delta^2}\right)^{\min(K, R_h)}.$$

Because $|\mathbf{w}|^2$ is Chi-square distributed, we obtain that [9, p. 25]

$$P\{|\mathbf{w}|^2 \geq aK\sigma_w^2\} = e^{-aK} \sum_{k=0}^{K-1} \frac{(2aK)^k}{k!} \leq c_K e^{-aK} a^K,$$

where $c_K = \sum_{k=0}^{K-1} \frac{(2K)^k}{k!}$ is a constant that only depends on K . By using G_d to represent $\min(K, R_h)$, Eq. (2.26) is simplified as :

$$P_e \leq c_h c_K \left(\frac{4K}{c_\delta^2}\right)^{G_d} \left(\frac{1}{\sigma_w^2}\right)^{-G_d} \left[\sum_{n=0}^{\infty} t^{n(K+G_d)} e^{-Kt^n}\right]. \quad (2.27)$$

It is not difficult to show that the summation (2.27) converges to a constant which only depends on K, t , and G_d when $t > 1$. Therefore, the diversity order of the LR-aided ZF equalizer is greater than or equal to $G_d = \min(K, R_h)$. However, as we know, the maximum diversity order for each group is $\min(K, R_h)$. Thus for LLP-OFDM, the LR-aided ZF equalizer collects diversity order $\min(K, R_h)$. ■

As we have shown, linear equalizers cannot exploit the multipath diversity for LLP-OFDM systems, however, after introducing the LR technique into the linear equalization process, multipath diversity is collected. Similar to the proof for Proposition 3, one can show that LR-aided MMSE estimator also collects multipath diversity. Note that LR-aided linear equalizers have some unique properties: i) the decoding complexity is much lower than ML and quite close to linear ones; ii) unlike SD, the complexity does not depend on SNR; iii) the complexity of CLLL part does not change along with constellation size.

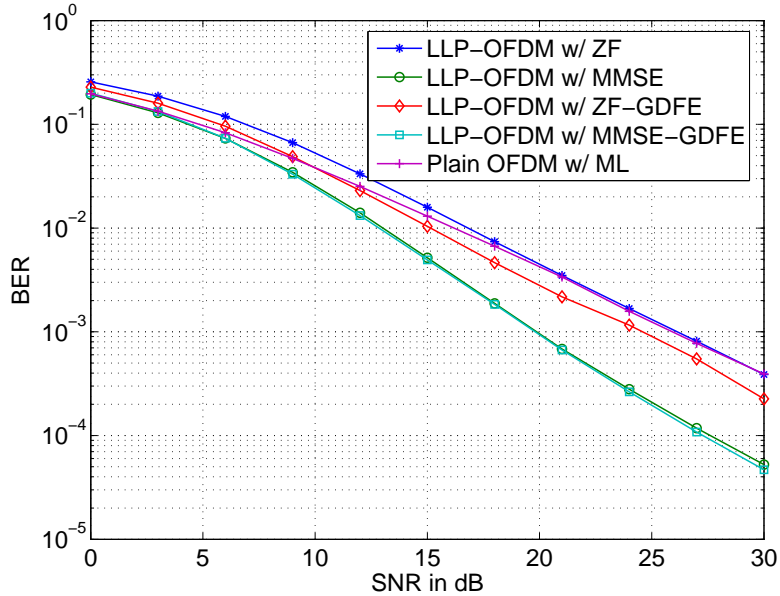


Figure 2.1: Comparisons among different linear equalizers

2.4 Simulation Results

In this section, we use computer simulations to verify our theoretical claims on the diversity order of linear equalizers and the performance of LR-aided linear equalizers.

Example 1 (Performance comparison of different equalizers): We first compare the performance of the LLP-OFDM with different equalizers with the conventional (plain) OFDM. We select $L = 3$, and the total subcarriers $N = 8$. The channel taps are i.i.d complex Gaussian random variables with zero mean and variance $\sigma^2 = 1/(L + 1)$. To enable the multipath diversity $G_d = L + 1 = 4$, we adopt the LLP-OFDM. The subcarriers are split into $N_g = 2$ groups with group size $K = 4$. QPSK modulation is used. The bit-error-rate (BER) versus SNR for linear equalizers is shown in Figure 2.1.

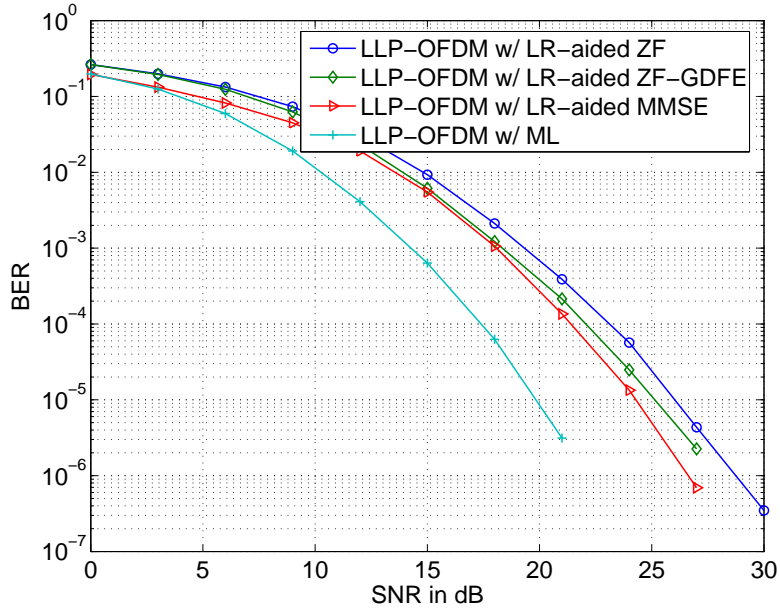


Figure 2.2: Comparisons among different equalizers for LLP-OFDM

For plain OFDM, we only consider symbol-by-symbol ML detection. For LLP-OFDM, we consider ZF, ZF-GDFE, MMSE, MMSE-GDFE. From Figure 2.1, we notice that: i) plain OFDM only achieves diversity one, and so do ZF, ZF-GDFE, MMSE and MMSE-GDFE detectors for LLP-OFDM; ii) for LLP-OFDM, the performance of ZF equalizer has the worst performance, while MMSE(-GDFE) has better performance than others. Figure 2.2 shows the BER curves of LR-aided ZF, LR-aided MMSE, LR-aided ZF-GDFE and ML detectors for LLP-OFDM. From this figure, we observe LR-aided ZF, MMSE or ZF-GDFE detectors of LLP-OFDM collect diversity order $L+1$ and so does ML detector. The performance of LR-aided MMSE equalizer is better than that of LR-aided ZF and ZF-GDFE, but there still exists a gap between the performance of LR-aided equalizers and ML detector. This is one of our future topics.

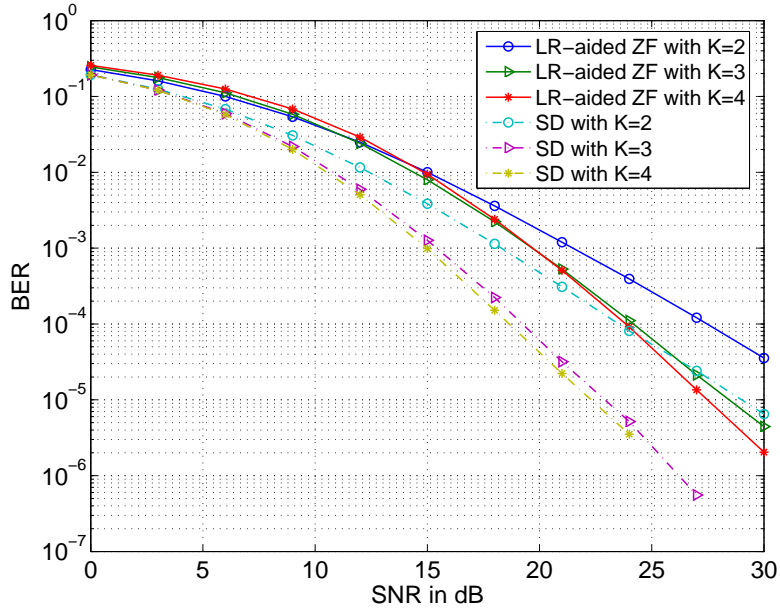


Figure 2.3: Comparisons among different group sizes using ML detector and complex LR-aided equalizer

Example 2 (Performance comparison of different group sizes): In this example, we fix the total number of subcarriers $N = 12$, channel order $L = 2$ and the number of total channel taps is $L + 1 = 3$. We use different group sizes to simulate the LLP-OFDM, and then compare the performance of them. The group size is chosen to be $K = 2, 3, 4$ respectively, and precoder Θ is designed according to [29]. At the receiver, both SD decoder and complex LR-aided ZF equalizer are employed and compared. Figure 2.3 shows the performance for different cases. Theoretically, the diversity order is $G_d = \min(K, L + 1)$ [12]. Based on the simulation results, we observe that the diversity order collected by both SD and complex LR-aided ZF equalizer is 2, 3 respectively corresponding to group size $K = 2, 3$. When $K = 4$, the channel taps in each group are

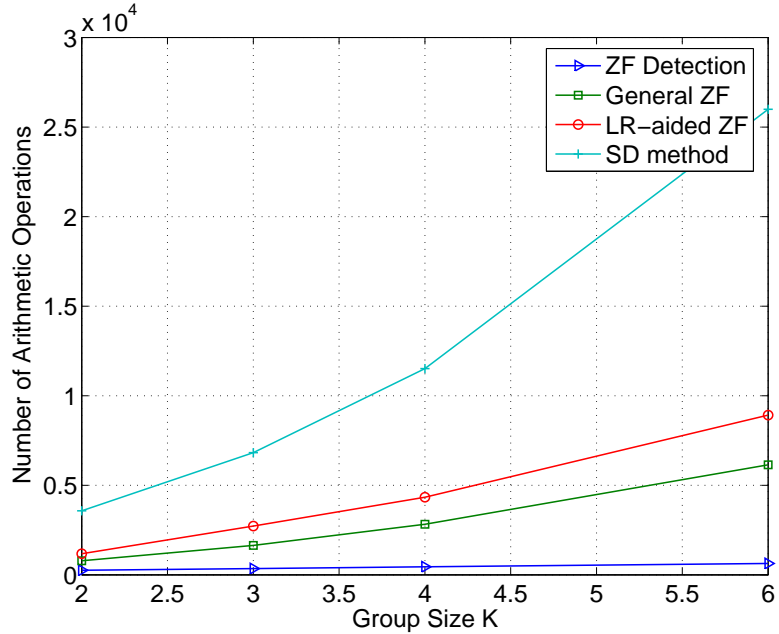


Figure 2.4: Complexity comparison of different decoding methods

correlated. We notice that our LR-aided linear equalizer still collects full diversity.

Example 3 (Complexity comparison of decoding schemes): After comparing the performance of different decoding methods with different group size, we verify here the difference of the complexity. Here, we choose the number of total sub-carriers of OFDM as $N = 12$ and the order of channel $L = 5$, then the multipath diversity order is 6. To compare the complexity of different decoding methods, we fix $SNR = 30dB$ and count the number of arithmetic operations (real additions and real multiplications). In Figure 2.4, we plot four curves to represent: SD method [7], complex LR-aided ZF equalizer, general ZF equalizer and ZF detection for LLP-OFDM. Here, general ZF detection means using pseudo-inverse equalizer $((\mathbf{D}_H \mathbf{\Theta})^{-1})$ and the simple ZF detection

is $\Theta^{\mathcal{H}} \mathbf{D}_H^{-1}$. From Figure 2.4, we notice that, the curve of LR-aided ZF equalizer is much closer to general ZF detection than to SD method. This means that the decoding complexity of LR-aided ZF is near that of general linear equalizers, and much lower than SD method. Furthermore, the ratio of the gap between LR-aided ZF and SD to the gap between LR-aided ZF and general ZF increases as group size K increases. Thus, LR-aided ZF equalizer becomes computational preferable as K increases. All of these four curves increase as K increases, which means the complexity increases as the group size increases while the performance is getting better. From Figure 2.4, we can see that the simplified ZF equalizer for LLP-OFDM is quite low but it can only collect diversity 1. However, with a complexity that is a little bit higher than ZF equalizer, LR-aided ZF equalizer can guarantee the same diversity as ML detector.

CHAPTER 3

LINEAR EQUALIZATION FOR V-BLAST SYSTEMS

In this chapter, we study the performance of V-BLAST multi-antenna architecture which is presented in [4] and [25]. Similar to the LLP-OFDM systems, through the analysis, we show that LR-aided linear equalizers can exploit the same diversity as ML detection while linear equalizers lose diversity which means performance degradation.

3.1 System Model of V-BLAST Systems

Consider a multi-antenna system with N_t transmit-antennas and N_r receive-antennas, where $N_r \geq N_t$. In V-BLAST model ([4, 25]), the data stream is divided into N_t sub-streams and transmitted through N_t antennas. These sub-streams consist of M -QAM symbols (or in general, symbols on Gaussian integer ring). For notation simplicity, we assume that the power of each transmit-antenna is normalized to one. Let $\mathbf{s} = [s_1, s_2, \dots, s_{N_t}]^T$ represents the $N_t \times 1$ transmitted data vector at one time slot, while $\mathbf{w} = [w_1, w_2, \dots, w_{N_r}]^T$ denotes the white Gaussian noise vector observed at the N_r receive-antennas with zero mean and variance σ_w^2 . Without any coding, we consider that $E\{\mathbf{s}\mathbf{s}^H\} = \mathbf{I}_{N_t}$ and $E\{\mathbf{w}\mathbf{w}^H\} = \sigma_w^2 \mathbf{I}_{N_r}$.

The received signal at one time slot is denoted as: $\mathbf{y} = [y_1, y_2, \dots, y_{N_r}]^T$ which is represented by:

$$\mathbf{y} = \mathbf{H}\mathbf{s} + \mathbf{w}, \quad (3.1)$$

where \mathbf{H} is the channel matrix, which consists of $N_r \times N_t$ uncorrelated complex Gaussian channel coefficients with zero mean and unit variance. We assume a flat-fading environment that the channel coefficients are constant during a frame and change independently from frame to frame. Also we assume that the channel matrix \mathbf{H} is known at the receiver.

Theoretically, at the receiver, we can perform maximum-likelihood (ML) detection to obtain the optimal performance of the system. Recall that the ML estimate is given as:

$$\hat{\mathbf{s}}_{ML} = \arg \min_{\mathbf{s} \in \mathcal{S}^{N_t}} \|\mathbf{y} - \mathbf{H}\mathbf{s}\|^2, \quad (3.2)$$

where $\|*\|$ denotes the 2-norm. The diversity order collected by an ML decoder for the system in (3.1) is N_r , the number of receive-antennas (see e.g., [28]). However, the cardinality of the searching space is $|\mathcal{S}^{N_t}| = M^{N_t}$, thus the exponential complexity prohibits the use of ML detection in practical systems (especially for systems that have large constellations and numbers of antennas). In the next section, we will introduce the linear detectors, whose decoding complexity is much lower than ML and thus computationally preferable in certain situation.

3.2 Linear Equalizers and Performance Analysis

In this section, we briefly describe the linear equalizers for V-BLAST systems and then focus on analyzing their performance.

3.2.1 ZF Equalizers

The zero-forcing (ZF) detector for the input-output relationship in (3.1) is given as:

$$\mathbf{x}_{ZF} = \mathbf{H}^\dagger \mathbf{y} = \mathbf{s} + \mathbf{H}^\dagger \mathbf{w} = \mathbf{s} + \mathbf{n}, \quad (3.3)$$

where \mathbf{H}^\dagger denotes the Moore-Penrose Pseudo-inverse of the channel matrix \mathbf{H} and $\mathbf{n} := \mathbf{H}^\dagger \mathbf{w}$ is the noise after equalization. The pseudo-inverse matrix can be written as :

$$\mathbf{H}^\dagger = (\mathbf{H}^H \mathbf{H})^{-1} \mathbf{H}^H \quad (3.4)$$

where the channel matrix \mathbf{H} has full column rank with probability one. Note that the noise vector \mathbf{n} is no longer white and its covariance matrix depends on the equalizer matrix \mathbf{H}^\dagger . The quantization step is then used to map each entry of \mathbf{x} into the symbol alphabet \mathcal{S} :

$$\hat{s}_n^{ZF} = \mathcal{Q}(x_n) = \arg \min_{s \in \mathcal{S}} |x_n - s|, \quad (3.5)$$

where x_n denotes the n th element of \mathbf{x}_{ZF} and $\mathcal{Q}(\cdot)$ means the quantizer of the symbol.

Starting from (3.3), we first study the performance of the ZF equalizer. Following the proof for Proposition 1 with $\mathbf{H}_{equ} = \mathbf{H}$, we can get the error probability given \mathbf{H} as:

$$P(s_i \rightarrow \tilde{s}_i | \mathbf{H}) = Q \left(\sqrt{\frac{|e_i|^2}{2\sigma_w^2 C_{ii}}} \right), \quad (3.6)$$

where C_{ii} is the (i, i) th element of \mathbf{C} and \mathbf{C} can be expressed as:

$$\mathbf{C} = \mathbf{H}^\dagger (\mathbf{H}^\dagger)^{\mathcal{H}} = (\mathbf{H}^{\mathcal{H}} \mathbf{H})^{-1}. \quad (3.7)$$

Based on (3.6), the diversity order collected by ZF equalizer is established in the following:

Proposition 4 *Given the model in (3.1), if the channels are i.i.d. complex Gaussian distributed, then the ZF equalizer in (3.3) exists with probability one and the diversity order for the system is $N_r - N_t + 1$.*

Proof: See Appendix D.

This proposition shows that not surprisingly, the ZF linear equalizer enables the same diversity as nulling-cancelling (NC) method for V-BLAST system [28], since NC method agrees with ZF equalizer when detecting the first symbol (the N_t th symbol of \mathbf{s}). However, the diversity order is lower than the ML equalizer.

3.2.2 MMSE Equalizers

Another type of linear equalizer is minimum mean square error (MMSE) detector which takes into account the noise variance. It minimizes the mean-square error between the actually transmitted symbols and the output of the linear detector and thus improves the performance. Given the model in (3.1), the MMSE equalizer is :

$$\mathbf{x}_{MMSE} = (\mathbf{H}^{\mathcal{H}} \mathbf{H} + \sigma_w^2 \mathbf{I}_{N_t})^{-1} \mathbf{H}^{\mathcal{H}} \mathbf{y}. \quad (3.8)$$

Again, the quantization step is the same as the one in (3.5). As shown in [26], with the definition of an extended system, the MMSE detector agrees with the ZF detector.

For the MMSE equalizer, we start from (3.8) and rewrite the system model as:

$$\mathbf{x}_{MMSE} = \mathbf{s} + (\mathbf{H}^H \mathbf{H} + \sigma_w^2 \mathbf{I}_{N_t})^{-1} (\mathbf{H}^H \mathbf{w} - \sigma_w^2 \mathbf{s}). \quad (3.9)$$

Define the equivalent noise vector $\mathbf{n} = (\mathbf{H}^H \mathbf{H} + \sigma_w^2 \mathbf{I}_{N_t})^{-1} (\mathbf{H}^H \mathbf{w} - \sigma_w^2 \mathbf{s})$. Given a signal vector \mathbf{s} , the noise vector \mathbf{n} has mean and covariance matrix, respectively as:

$$\begin{aligned} \bar{\mathbf{n}} &= -\sigma_w^2 (\mathbf{H}^H \mathbf{H} + \sigma_w^2 \mathbf{I}_{N_t})^{-1} \mathbf{s} \\ \mathbf{\Sigma} &= \sigma_w^2 (\mathbf{H}^H \mathbf{H} + \sigma_w^2 \mathbf{I}_{N_t})^{-1} - \sigma_w^4 (\mathbf{H}^H \mathbf{H} + \sigma_w^2 \mathbf{I}_{N_t})^{-2}. \end{aligned} \quad (3.10)$$

Similar to the analysis for the ZF equalizer, we can verify that error probability is given as:

$$P(s_i \rightarrow \tilde{s}_i | \mathbf{H}) = Q \left(\sqrt{\frac{(|e_i|^2 + e_i^* \bar{n}_i + e_i \bar{n}_i^*)^2}{2|e_i|^2 \Sigma_{ii}}} \right), \quad (3.11)$$

where \bar{n}_i is the i th element of noise mean $\bar{\mathbf{n}}$ and Σ_{ii} is the (i, i) th element of noise covariance matrix $\mathbf{\Sigma}$ in (3.10). At high signal-to-noise ratio (SNR), i.e., when σ_w^2 is much smaller than 1, Eq. (3.11) can be approximated as:

$$P(s_i \rightarrow \tilde{s}_i | \mathbf{H}) \approx Q \left(\sqrt{\frac{|e_i|^2}{2\sigma_w^2 \tilde{C}_{ii}}} \right), \quad (3.12)$$

where \tilde{C}_{ii} is the (i, i) th element of $(\mathbf{H}^H \mathbf{H} + \sigma_w^2 \mathbf{I}_{N_t})^{-1}$. It is ready to verify that \tilde{C}_{ii} has the same degrees of freedom as C_{ii} in (3.6). This shows that MMSE detector can achieve the same diversity as ZF detector:

Proposition 5 *Given the model in (3.1), if the channels are i.i.d. complex Gaussian distributed, then MMSE equalizer in (3.8) exists with probability one and the diversity order for the system is $N_r - N_t + 1$.*

In general, the MMSE equalizer outperforms the ZF equalizer with larger coding advantage because \tilde{C}_{ii} is always less than C_{ii} . Furthermore, if we spell out \tilde{C}_{ii} and C_{ii} , for the same SNR, as the number of receive-antennas (N_r) increases, the performance gap between MMSE and ZF detectors decreases. In [21], it has been shown that certain linear precoded OFDM systems can also achieve maximum diversity by linear equalizers. However, here we have shown that linear equalizers for V-BLAST systems can only achieve diversity order $N_r - N_t + 1$, which is less than the maximum diversity N_r . In the following, we show that using lattice reduction methods, we can restore the maximum diversity order N_r .

3.3 LR-Aided Linear Equalizers

The performance of LR-aided linear detectors for V-BLAST system is established in the following proposition:

Proposition 6 *The diversity order collected by a Lattice-Reduction aided linear detector (LR-aided ZF or LR-aided MMSE) for an MIMO V-BLAST system with N_t transmit-antennas and N_r receive-antennas is N_r , which is the same as that obtained by maximum-likelihood detector.*

The proof is similar to that of Proposition 3. What we need to prove is $P\{|\mathbf{h}_{min}| \leq \epsilon\} \leq c_h \epsilon^{2N_r}$, where \mathbf{h}_{min} is the vector with the minimum norm of all the vectors in the lattice spanned by \mathbf{H} . Since all the entries of \mathbf{H} are i.i.d. complex Gaussian random variables with zero-mean, the rank of $E[\mathbf{h}_n \mathbf{h}_n^H]$ is N_r for $n \in [1, N_t]$. Furthermore, the N_t columns are linear independent with each other on the Gaussian integer ring with probability one. Thus, according to Corollary 1, we can obtain that $P\{|\mathbf{h}_{min}| \leq \epsilon\} \leq c_h \epsilon^{2N_r}$. Then following the proof of Proposition 3, we can see, for V-BLAST systems LR-aided ZF equalizer can collect diversity N_r , which is the same as that exploited by ML detection.

3.4 Simulation Results

In this section, we use computer simulations to verify our theoretical claims on the diversity order of linear equalizers and the performance of LR-aided linear equalizers for V-BLAST systems. The channels are generated as i.i.d. complex Gaussian variables with zero mean and unit variance. The SNR is defined as symbol energy per transmit-antenna versus noise power.

Example 1 (Diversity collected by linear equalizers): The ZF and MMSE equalizers in (3.3) and (3.8) are considered for V-BLAST systems in this example. We consider $N_t = 2$ transmit-antennas, and different numbers of receive-antennas $N_r = 2, 3, 4$. BPSK is used as the modulation scheme. The bit-error rate (BER) versus SNR is depicted in Figure 3.1. Reading the slopes of the curves in Figure 3.1, we observe that the diversity orders enabled by either ZF or MMSE equalizer are indeed $N_r - N_t + 1$, which in this

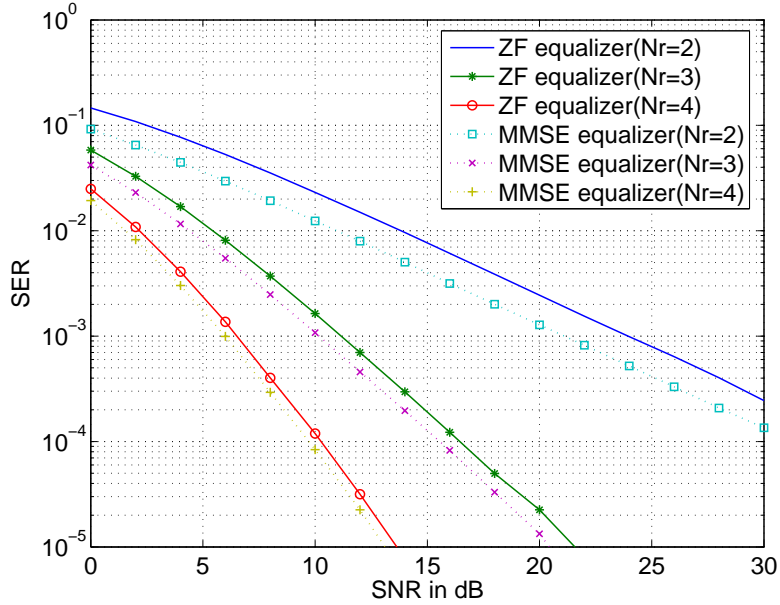


Figure 3.1: BER of systems with $N_t = 2$ and $N_r = 2, 3, 4$ separately and BPSK modulation

example are 1, 2, and 3. Furthermore, we observe that the performance of MMSE detection is better than ZF detection and the gap between them decreases as N_r increases.

Example 2 (LR-aided linear equalizers): In this example, we fix the number of transmit- and receive-antennas as $N_t = 3, N_r = 4$, and use QPSK as the modulation scheme. Five detection methods are applied to the system: ZF detection, MMSE detection, complex LR-aided ZF detection, complex LR-aided MMSE detection and ML detection. Observing Figure 3.2, we notice that the linear detectors can only achieve the diversity order $N_r - N_t + 1$ which is 2 in this case. The ML detector enables diversity order $N_r = 4$. As expected, the LR-aided linear detectors achieve the same diversity order as the ML does. The performance gap between LR-aided linear detectors and ML

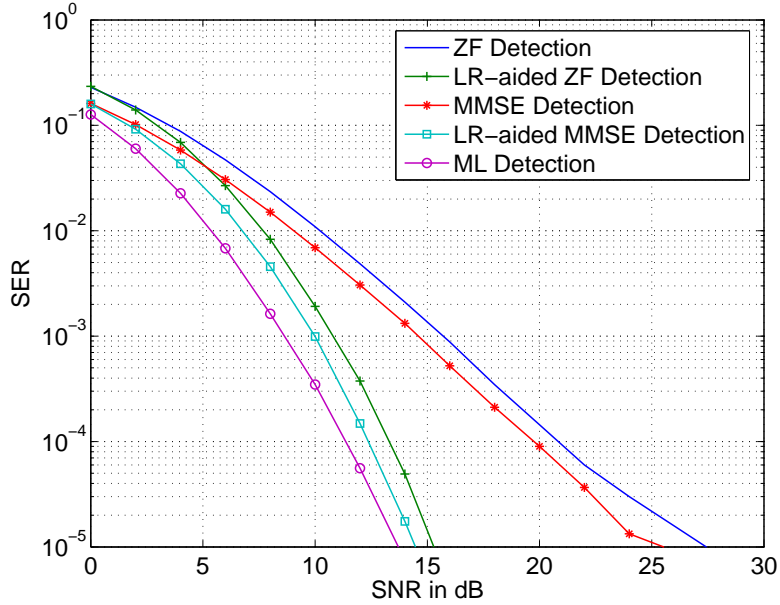


Figure 3.2: SER of a system with $(N_t, N_r) = (3, 4)$ and QPSK modulation

detector is because the LLL algorithm cannot perfectly diagonalize the channel matrix.

Example 3 (Complex LLL algorithm): As shown in Chapter 2, we have extended the LLL algorithm to complex field for any number of transmit-antenna. The detailed CLLL algorithm can be found in Appendix B. In this example, we compare the complex LLL algorithm with the real LLL algorithm in terms of complexity and performance. The arithmetic operations we count are the number of real additions and real multiplications. In Figure 3.3, we count the average number of arithmetic operations needed by the complex and real LLL algorithm separately as $N_r = N_t = n$ increases. We can see that the complexity of the real LLL algorithm is about $\mathcal{O}(n^4)$ which is consistent with the result in [10]. The number of arithmetic operations that the real LLL algorithm

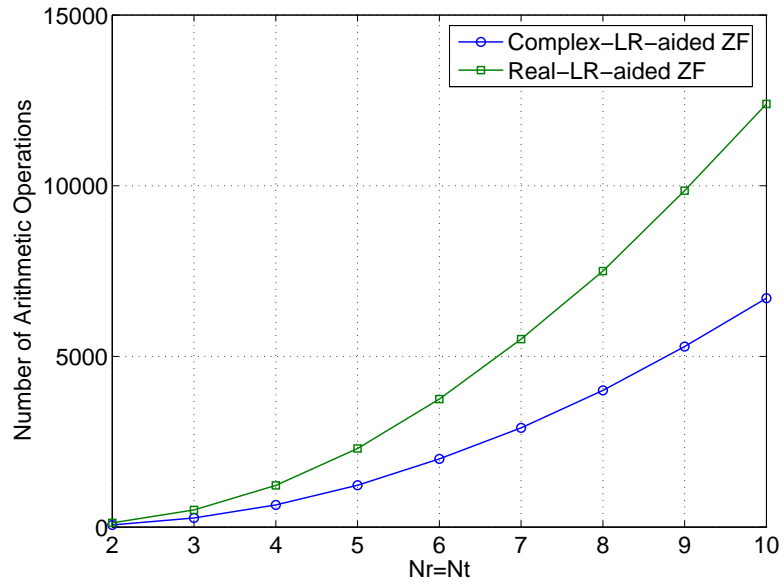


Figure 3.3: Complexity comparison between complex LLL and real LLL algorithms

needs is about 1.5 times of that of the complex LLL algorithm. Therefore, the complex LLL algorithm is more efficient. In Figure 3.4, we also compare the performance of complex LR-aided and real LR-aided schemes. It can be seen that complex LR-aided linear equalizers have the same performance as the real ones. So we can see, with lower complexity and the same performance, complex LLL algorithm is computational preferable to real LLL algorithm.

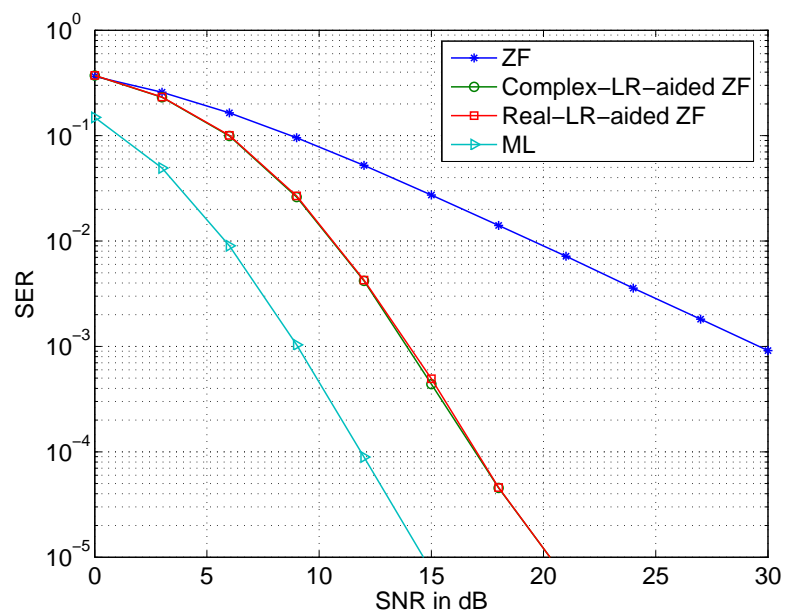


Figure 3.4: Performance comparison between the complex and real LLL algorithms with $(N_t, N_r) = (4, 4)$

CHAPTER 4

EXTENSION TO MIMO-OFDM SYSTEMS

As we have shown, linear equalizers can not exploit the multipath diversity for LLP-OFDM systems, however, after introducing the LR technique into the linear equalization process, multipath diversity is collected. In this chapter, we see similar situation happens to the MIMO-OFDM designs. The block diagram of MIMO-OFDM is depicted in Fig.4.1. There are N_r receive-antennas and N_t transmit-antennas, and the frequency-selective wireless links between transmit- and receive-antennas have the same channel order L . The channel taps of the link between the μ th transmit-antenna and the ν th receive-antenna are denoted as $h_l^{(\nu,\mu)}$ for $l \in [0, L]$ and $\nu \in [1, N_r], \mu \in [1, N_t]$. $x_n^\mu(p)$ represents the symbol transmitted on the p th subcarrier from the μ th transmit-antenna in the n th OFDM time slot while $y_n^\nu(p)$ is received at the ν th receive-antenna on the p th subcarrier in the n th OFDM slot.

There are many coding schemes designed for MIMO-OFDM and different designs will present different performance even with the same equalizers. In this section, we will use two coding schemes: full-diversity-full-rate (FDFR) design in [13] and space-time-frequency (STF) design in [11] as examples to show the diversity that linear equalizers and LR-aided linear detection methods can collect.

4.1 FDFR-OFDM

Multi-antenna systems not only provide space diversity, but also boost transmission rate. FDFR design has been introduced to enjoy both advantages [13]. When channels

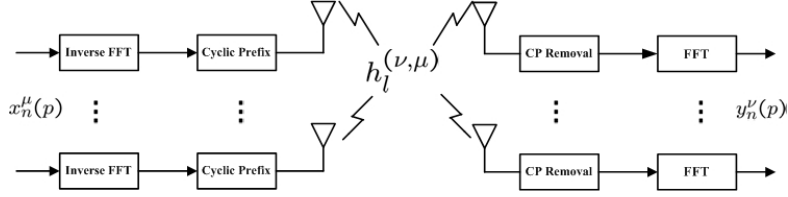


Figure 4.1: Block Diagram of MIMO-OFDM

are frequency-selective, FDFR design can be combined with OFDM to reduce the equalization complexity and collect diversity to combat fading. However, the main price paid here is decoding complexity (see [13] for details). In the following, we briefly introduce the FDFR-OFDM design and then give the performance analysis when linear equalizers or LR-aided equalizers are employed.

Let $\mathbf{y}(p) \in \mathbb{C}^{N_r \times 1}$ represent the symbol vector received through N_r receive-antennas on the p th subcarrier. By stacking $\mathbf{y}(p), p \in [0, N_c - 1]$ (N_c is the number of total subcarriers which we assume to be $N_t(L + 1)$ for simplicity) into one symbol vector, the I/O relationship of FDFR design is represented as:

$$\begin{bmatrix} \mathbf{y}(0) \\ \vdots \\ \mathbf{y}(N_c - 1) \end{bmatrix} = \begin{bmatrix} \mathbf{H}(0)(\mathbf{P}_1 \mathbf{D}_\beta) \otimes \boldsymbol{\theta}_1^T \\ \vdots \\ \mathbf{H}(N_c - 1)(\mathbf{P}_{N_t} \mathbf{D}_\beta) \otimes \boldsymbol{\theta}_{N_c}^T \end{bmatrix} \mathbf{s} + \begin{bmatrix} \mathbf{w}(0) \\ \vdots \\ \mathbf{w}(N_c - 1) \end{bmatrix} = \mathbf{H}_{FDFR} \mathbf{s} + \mathbf{w}, \quad (4.1)$$

where the permutation matrix \mathbf{P}_n and the diagonal matrix \mathbf{D}_β are defined as:

$$\mathbf{P}_n := \begin{bmatrix} \mathbf{0} & \mathbf{I}_{n-1} \\ \mathbf{I}_{N_t-n+1} & \mathbf{0} \end{bmatrix}, \quad \mathbf{D}_\beta := \text{diag}[1, \beta, \dots, \beta^{N_t-1}], \quad (4.2)$$

and scalar β can be found in [13], $\mathbf{H}(p), p \in [0, N_c - 1]$ is the MIMO channel matrix on the $(p + 1)$ st sub-carrier with the (ν, μ) th entry $H^{(\nu, \mu)}(p) = \sum_{l=0}^L h_l^{(\nu, \mu)} e^{-j \frac{2\pi p l}{N_c}}$, $\boldsymbol{\theta}_n^T$ is the n th row of $N_c \times N_c$ LCF encoding matrix $\boldsymbol{\Theta}$ and \mathbf{s} comprises $N_t^2(L + 1)$ symbols. Based on this system model, we first summarize the results for FDFR design as follows:

Proposition 7 *Considering an FDFR-OFDM system with N_t transmit-antennas and N_r receive-antennas, and the frequency-selective channel order of L , given the model in (4.1), if the channel taps are independently complex Gaussian distributed with zero mean, then the ZF equalizer exists wp1 and collects diversity order $N_r - N_t + 1$. An LR-aided ZF equalizer exists wp1 and collects full diversity $N_r N_t(L + 1)$ which is the same as that exploited by ML detector.*

According to the design of β and $\boldsymbol{\Theta}$ in [13] and the structure of \mathbf{H}_{FDFR} , it is not difficult to verify that \mathbf{H}_{FDFR} has full rank wp1, which means ZF equalizer exists wp1 for the model given in (4.1). Following the general proof of Proposition 1, we can express the error probability of the FDFR design using ZF equalizer as:

$$P(s_i \rightarrow \tilde{s}_i | \mathbf{H}_{FDFR}) = Q \left(\sqrt{\frac{|e_i|^2}{2\sigma_w^2 C_{ii}}} \right). \quad (4.3)$$

where C_{ii} is the (i, i) th entry of the matrix $\mathbf{C} = (\mathbf{H}_{FDFR}^H \mathbf{H}_{FDFR})^{-1}$. Given \mathbf{H}_{FDFR} as in (4.1) we can get the specific form of C_{ii} as:

$$C_{ii} = \frac{1}{N_c} \sum_{p=0}^{N_c-1} C_{kk}(p) = \frac{1}{N_c} \sum_{p=0}^{N_c-1} \frac{1}{C_{kk}^{-1}(p)}, \quad k = (m + p) - \left(\left\lceil \frac{m + p}{N_t} \right\rceil - 1 \right) N_t \quad (4.4)$$

where $m = \left\lceil \frac{i}{N_c} \right\rceil$ and $C_{kk}(p)$ is the (k, k) th entry of the matrix $\mathbf{C}(p) = (\mathbf{H}^H(p)\mathbf{H}(p))^{-1}$.

Thus, we can bound C_{ii} as:

$$\frac{1}{N_c C_{k_c k_c}^{-1}(c)} \leq C_{ii} \leq \frac{1}{\min_{0 \leq p \leq N_c - 1} C_{kk}^{-1}(p)} \quad (4.5)$$

Here c is a constant number, $c \in [0, N_c - 1]$ and k_c is determined by c and i . As stated in Appendix. D, $C_{kk}^{-1}(p)$ is a Chi-square random variable with degrees of freedom of $2(N_r - N_t + 1)$. With the error probability expressed in (4.3), by using Lemma 1, the outage probability can be bounded as:

$$\frac{(N_r - N_t + 1)^{N_r - N_t}}{\Gamma(N_r - N_t + 1)} \left(\frac{2\sigma_w^2 \gamma^{th}}{N_c |e_i|^2} \right)^{N_r - N_t + 1} \leq P(\gamma < \gamma^{th}) \leq c_u \left(\frac{2\sigma_w^2 \gamma^{th}}{|e_i|^2} \right)^{N_r - N_t + 1}. \quad (4.6)$$

So we can obtain that the diversity order of ZF equalizer for FDFR design is $N_r - N_t + 1$.

Regarding the performance of LR-aided ZF equalizer for FDFR designs, the proof is similar to that for Proposition 3. We only need to prove $P\{|\mathbf{h}_{min}|^2 \leq \epsilon\} \leq c_h \epsilon^{N_r N_t (L+1)}$, where \mathbf{h}_{min} is the vector with minimum non-zero norm of all the vectors in the lattice spanned by \mathbf{H}_{FDFR} . Given the system in (4.1), we can write the specific form of the i th column of \mathbf{H}_{FDFR} as :

$$\mathbf{h}_i = \begin{bmatrix} \mathbf{H}(0)_m \beta^{(m-1)} \Theta_{1, i-(m-1)N_c} \\ \vdots \\ \mathbf{H}(p)_{(p+m)-(n-1)N_t} \beta^{(m-1)} \Theta_{p+1, i-(m-1)N_c} \\ \vdots \\ \mathbf{H}(N_c - 1)_{(N_c+m)-(n-1)N_t} \beta^{(m-1)} \Theta_{N_c, i-(m-1)N_c} \end{bmatrix}, \quad (4.7)$$

where $m = \lceil \frac{i}{N_c} \rceil$ and $n = \lceil \frac{m+p}{N_t} \rceil$. $\mathbf{H}(p)_{(p+m)-(n-1)N_t}$ is the $((p+m) - (n-1)N_t)$ th column of the matrix $\mathbf{H}(p)$, and $\Theta_{p+1, i-(m-1)N_c}$ is the $(p+1, i-(m-1)N_c)$ th entry of the LCF encoder Θ . Since $\beta^{(m-1)}\Theta_{p+1, i-(m-1)N_c}$ is deterministic given i and p , the statistical property of the i th column is determined by $\mathbf{H}(p)_{(p+m)-(n-1)N_t}, p \in [0, N_c-1]$, which is the frequency response of the p th subcarrier of the frequency-selective channels between the $((p+m) - (n-1)N_t)$ th transmit-antenna and N_r receive-antennas. Intuitively, the $N_r N_t (L+1) \times 1$ vector \mathbf{h}_i selects $L+1$ subcarriers from each of the total $N_r N_t$ frequency-selective channels. So the rank of the covariance matrix of each column is $N_r N_t (L+1)$. The $N_t^2 (L+1)$ columns are linear independent with each other which is guaranteed by the LCF encoder Θ and the choice of β in [13]. Thus, similar to LLP-OFDM, following the proof of Proposition 3, we can get that the diversity order of the LR-aided linear equalizer for FDFR design is $N_r N_t (L+1)$ which is also the maximum diversity order that the system can achieve.

4.2 STF-OFDM

STF design is also composed of two stages: LCF encoding across subcarriers and ST multiplexing using ST orthogonal code [20]. For example, when $N_t = 2$, the $2N_g K \times 1$ symbol vector \mathbf{s} is split into $2N_g$ groups, $\mathbf{s}_n \in \mathbb{C}^{K \times 1}, n \in [1, 2N_g]$. Then, we transmit every two groups through two transmit-antennas using Alamouti scheme [2] after encoding the symbol blocks \mathbf{s}_n with the $K \times K$ LCF encoding matrix Θ . The I/O relationship

for each group is:

$$\begin{bmatrix} y_n(0) \\ \vdots \\ y_n(K-1) \end{bmatrix} = \begin{bmatrix} |\mathbf{H}(0)| & & \\ & \ddots & \\ & & |\mathbf{H}(K-1)| \end{bmatrix} \Theta \mathbf{s}_n + \hat{\mathbf{w}} = \mathbf{H}_{STF} \mathbf{s}_n + \hat{\mathbf{w}}. \quad (4.8)$$

where $\hat{\mathbf{w}}$ is the equivalent white Gaussian noise vector, and

$$|\mathbf{H}(p)|^2 = \sum_{\nu=1}^{N_r} \sum_{\mu=1}^{N_t} |H^{(\nu,\mu)}(p)|^2 = \sum_{\nu=1}^{N_r} \sum_{\mu=1}^{N_t} \left| \sum_{l=0}^L h_l^{(\nu,\mu)} e^{-j\frac{2\pi p}{K}l} \right|^2. \quad (4.9)$$

Based on this system model in (4.8), we apply the ML detection or SD method to get the estimation of information symbols $\hat{\mathbf{s}}_n$. According to [11], when the group length K is greater than or equal to $L+1$, these optimal and near optimal detectors exploit the full diversity $N_r N_t (L+1)$.

Given the model in (4.8), we can see that the ZF equalizer for the STF design exists with probability one. Since (4.8) has the same form as (2.2), we can get the error probability as in (2.7), where C_{ii} now is the (i, i) th entry of the matrix $\mathbf{C} = (\mathbf{H}_{STF}^H \mathbf{H}_{STF})^{-1}$. Similarly, we can bound C_{ii} as:

$$\frac{1}{K} \frac{1}{|\mathbf{H}(c)|^2} \leq C_{ii} = \frac{1}{K} \sum_{k=0}^{K-1} \frac{1}{|\mathbf{H}(k)|^2} \leq \frac{1}{\min_{0 \leq k \leq K-1} |\mathbf{H}(k)|^2}, \quad (4.10)$$

where c is a constant in $[0, K-1]$. Since $|\mathbf{H}(p)|^2$ is the summation of $N_r N_t$ independent Chi-square random variable with degrees of freedom 2 as shown in (4.9), according to [15], $|\mathbf{H}(p)|^2$ still performs like a Chi-square random variable with degrees of freedom

$2N_r N_t$. Following the proof of Proposition 3, we can bound the outage probability as:

$$\frac{(N_r N_t)^{N_r N_t - 1}}{\Gamma(N_r N_t)} \left(\frac{2\sigma_w^2 \gamma^{th}}{K|e_i|^2} \right)^{N_r N_t} \leq P(\gamma < \gamma^{th}) \leq c_u \left(\frac{2\sigma_w^2 \gamma^{th}}{|e_i|^2} \right)^{N_r N_t} \quad (4.11)$$

So, the diversity order that the ZF equalizer can exploit for STF design is $N_r N_t$.

To show that the diversity order collected by LR-aided ZF equalizer for STF design is $N_r N_t(L + 1)$, we need to show for the lattice spanned by \mathbf{H}_{STF} , $P\{|\mathbf{h}_{min}|^2 \leq \epsilon\} \leq c_h \epsilon^{N_r N_t(L+1)}$, where \mathbf{h}_{min} is the vector with minimum non-zero norm of all the vectors in the lattice. In other words we need to make sure the three conditions in Corollary 1 are satisfied. Obviously, all the entries in \mathbf{H}_{STF} are complex Gaussian distributed with zero mean. From (4.8), we can see that the k th column of the equivalent channel matrix \mathbf{H}_{STF} of the system is $\mathbf{h}_k = \text{diag}[|\mathbf{H}(0)|, \dots, |\mathbf{H}(K-1)|] \boldsymbol{\theta}_k, k \in [1, K]$, the square norm of which is a Chi-square random variable with degrees of freedom $2N_r N_t(L + 1)$, where $\boldsymbol{\theta}_k$ is the k th column of $\boldsymbol{\Theta}$. Further, because of the linear independence of LCF encoding matrix $\boldsymbol{\Theta}$, all the columns of the equivalent channel matrix \mathbf{H}_{STF} are linear independent with each other. So according to Corollary 1, we have $P\{|\mathbf{h}_{min}| \leq \epsilon\} \leq c_h \epsilon^{2N_r N_t(L+1)}$. Thus, following the proof of Proposition 3, we can get that the diversity order of LR-aided ZF equalizer for STF design is $N_r N_t(L + 1)$. The results for STF design are summarized in the following proposition:

Proposition 8 *Consider an STF-OFDM system with N_t transmit-antennas and N_r receive-antennas, and the frequency-selective channel order of L . Given the model in (4.8), if the channel taps are independently complex Gaussian distributed with zero mean, then ZF equalizer in (2.3) exists wp1 and exploits diversity order $N_r N_t$. For STF design,*

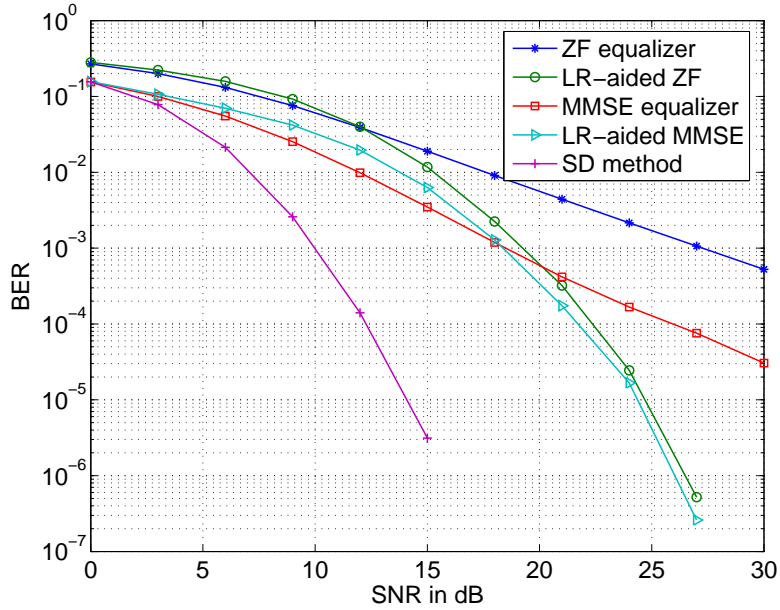


Figure 4.2: Comparison among different equalizers for FDFR design

an LR-aided ZF equalizer collects diversity order $N_r N_t (L + 1)$ which is the same as that obtained by ML detector.

4.3 Simulation Results

Example 1 (Performance comparison of different equalizers for FDFR): Consider a multiantenna system with $N_t = N_r = 2$ and frequency-selective channel order $L = 1$. Five detectors are employed respectively on model (4.1): ZF, MMSE, LR-aided ZF, LR-aided MMSE detectors and sphere decoder (SD). QPSK modulation is used for modulation. The BER versus SNR performance is depicted in Figure 4.2. It shows that the linear detectors (ZF, MMSE) can only achieve diversity $N_r - N_t + 1 = 1$. However, the LR-aided linear detectors achieve maximum diversity $N_r N_t (L + 1) = 8$ with

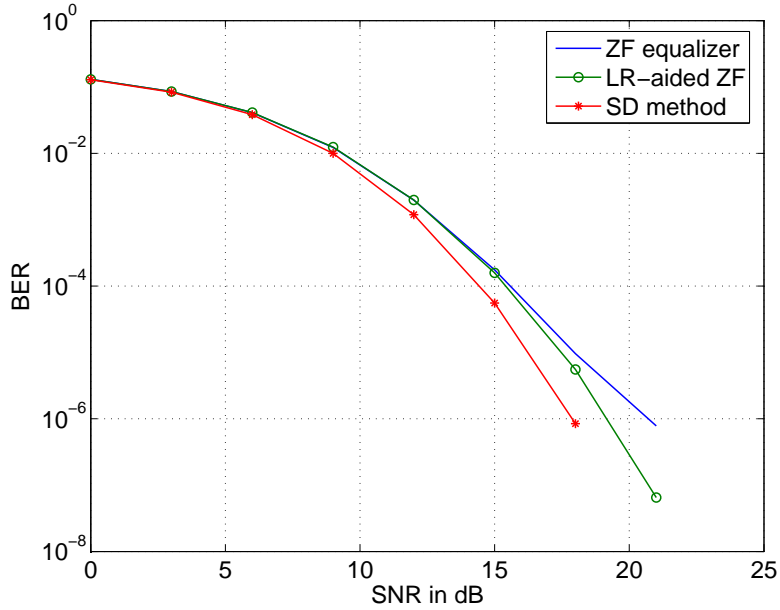


Figure 4.3: Comparison among different equalizers for STF design

much lower complexity than the SD detector though there exists a gap between SD and LR-aided linear detectors.

Example 2 (Performance comparison of different equalizers for STF): STF design is simulated and 16-QAM is chosen as symbol modulation scheme. We use the channel configuration in previous example. ZF, LR-aided ZF and SD equalizers are applied to the system model in (4.8). Performance of different equalizers is plotted in Figure 4.3. Reading the slopes of the curves in Figure 4.3, we observe that the diversity orders for ZF equalizer is indeed $N_r N_t = 4$ while LR-aided ZF equalizer can achieve maximum diversity $N_r N_t (L + 1) = 8$, the same as SD. Note that Figure 4.3 also shows that if the spatial diversity order ($N_t N_r$) is high, linear equalizers achieve similar performance as SD for a large SNR range.

CHAPTER 5

CONCLUDING REMARKS AND FUTURE RESEARCH DIRECTIONS

In this thesis, we have discussed the performance in terms of diversity of linear detectors for LLP-OFDM systems, V-BLAST systems and two MIMO-OFDM designs. It shows that conventional linear equalizers can only collect diversity 1 for LLP-OFDM systems and $N_r - N_t + 1$ for V-BLAST systems though they have the lowest complexity. For MIMO-OFDM designs, it depends on the ST coding schemes. However, with slightly increased complexity, LR-aided linear equalizers achieve maximum diversity for LLP-OFDM, V-BLAST and MIMO-OFDM designs, which is the same as that collected by ML detector. The complexity of LR-aided linear equalizers is much lower than those of ML and near-ML detectors.

Based on this thesis, future research directions are listed but not limited as follows:

First, the performance analysis in terms of coding gain will be studied. Based on our simulation results, it has been shown that although LR-aided equalizers achieve the same diversity as ML does, there still exists a performance gap which is mainly due to coding gain loss. In this research thrust, we will first quantify the coding gain of LR-aided linear equalizers and then try to modify the equalizers to reduce the performance gap with ML. Furthermore, we will study the performance of coded linear systems with LR-aided decoding and compare the performance and complexity with other alternatives in the literature.

Another future research direction is the study of the orthogonality deficiency of the equivalent channel matrix for wireless communications. As we know, for linear systems,

when the equivalent channel matrix is diagonal, the performance of ZF equalizer is the same as that of ML detector. However, in general the channel matrix \mathbf{H}_{equ} is not diagonal, and thus linear equalizers have inferior performance. Orthogonality deficiency describes how “diagonal” a matrix is. So the study of orthogonality deficiency provides a useful tool to quantify the diversity and coding gains of linear equalizers. Furthermore, how it will affect the performance of linear equalizations may guide us to construct the coding schemes to reach full diversity and high coding gain when linear equalizers are adopted at the receiver. Hybrid equalizers will also be designed to trade-off the performance with complexity.

BIBLIOGRAPHY

- [1] E. Agrell, T. Eriksson, A. Vardy and K. Zeger, “Closest point search in lattices,” *IEEE Trans. on Information Theory*, vol. 48, no. 8, pp. 2201–2214, Aug. 2002.
- [2] S. M. Alamouti, “A simple transmit diversity technique for wireless communications,” *IEEE Journal on Selected Areas in Communications*, vol. 16, no. 8, pp. 1451–1458, Oct. 1998.
- [3] J. A. C. Bingham, “Multicarrier modulation for data transmission: an idea whose time has come,” *IEEE Communications Magazine*, vol. 28, no. 5, pp. 5–14, May. 1990.
- [4] G. J. Foschini, “Layered space-time architecture for wireless communication in a fading environment when using multiple antennas,” *Bell Labs Technical Journal*, vol. 1, no. 2, pp 41-59, Autumn 1996.
- [5] G. Ginis and J. M. Cioffi, “On the relationship between V-BLAST and the GDFE,” *IEEE Communications Letters*, vol. 5, pp. 364–366, Sept. 2001.
- [6] G. D. Golden, C. J. Foschini, R. A. Valenzuela and P. W. Wolniansky, “Detection algorithm and initial laboratory results using V-BLAST space-time communication architecture,” *Electronics Letters*, vol. 35, no. 1, pp. 14–16, Jan. 1999.
- [7] B. Hassibi and H. Vikalo, “On the sphere-decoding algorithm I. Expected complexity,” *IEEE Trans. on Signal Processing*, vol. 53, no. 8, pp. 2806–2818, Aug. 2005.
- [8] Y. Huan and G. W. Wornell, “Lattice-reduction-aided detectors for MIMO communication systems,” *Proc. of IEEE Global Telecommunications Conf.*, vol. 1, pp. 424–428, Nov. 17-21, 2002.
- [9] S. Kay, *Fundamentals of statistical signal processing: Detection Theory*, Vol. II, Prentice Hall, 1998.
- [10] A. K. Lenstra, H. W. Lenstra and L. Lovász, “Factoring polynomials with rational coefficients,” *Math. Ann.*, vol. 261, pp. 515–534, 1982.
- [11] Z. Liu, Y. Xin and G. B. Giannakis, “Space-time-frequency coded OFDM over frequency-selective fading channels,” *IEEE Trans. on Signal Processing*, vol. 50, no. 10, pp. 2465–2476, Oct. 2002.
- [12] X. Ma and G. B. Giannakis, “Complex field coded MIMO systems: performance, rate, and tradeoffs,” *Wireless Communications and Mobile Computing*, pp. 693-717, Nov. 2002.

- [13] X. Ma and G. B. Giannakis, "Full-diversity full-rate complex-field space-time coding," *IEEE Trans. on Signal Processing*, vol. 51, no. 11, pp. 2917-2930, Nov. 2003.
- [14] W. H. Mow, "Universal lattice decoding: a review and some recent results," *Proc. of IEEE International Conf. on Communications*, vol. 5, pp. 2842 - 2846, Jun. 20-24, 2004.
- [15] A. Papoulis and U. S. Pillai, *Probability, random variables and stochastic processes*, McGraw-Hill Science/Engineering/Math, 4th edition, 2001.
- [16] H. V. Poor and S. Verdù, "Probability of error in MMSE multiuser detection," *IEEE Trans. on Information Theory*, vol. 43, no. 3, pp. 858-871, May. 1997.
- [17] J. G. Proakis, "Digital Communications," McGraw-Hill, 4th edition, 2000.
- [18] V. Tarokh, N. Seshadri and A. R. Calderbank, "Space-time codes for high data rate wireless communication: performance criterion and code construction," *IEEE Trans. on Information Theory*, vol. 44, no. 2, pp. 744-765, Mar. 1998.
- [19] M. Taherzadeh, A. Mobasher and A. K. Khandani, "Lattice-basis reduction achieves the precoding diversity in MIMO broadcast systems," *Proc. of the 39th Conf. on Information Sciences and Systems*, Johns Hopkins Univ., MD, Mar. 15-18, 2005.
- [20] V. Tarokh, H. Jafarkhani and A. R. Calderbank, "Space-time block coding for wireless communications: performance results," *IEEE Journal of Selected Areas*, vol. 17, no. 3, pp. 451-460, Mar. 1999.
- [21] C. Tepedelenlioglu, "Maximum multipath diversity with linear equalization in precoded OFDM systems," *IEEE Trans. on Information Theory*, vol. 50, no. 1, pp. 232-235, Jan. 2004.
- [22] Z. Wang and G. B. Giannakis, "Complex-field coding for OFDM over fading wireless channels," *IEEE Trans. on Information Theory*, vol. 49, no. 3, pp. 707-720, Mar. 2003.
- [23] Z. Wang and G. B. Giannakis, "A simple and general parameterization quantifying performance in fading channels," *IEEE Trans. on Communications*, vol. 51, no. 8, pp. 1389-1398, Aug. 2003.
- [24] C. Windpassinger and R. F. H. Fischer, "Low-complexity near-maximum-likelihood detection and precoding for MIMO systems using lattice reduction," *Proc. of Information Theory Workshop*, pp. 345-348, Mar. 31-Apr. 4, 2003.
- [25] P. W. Wolniansky, G. J. Foschini, G. D. Golden and R. A. Valenzuela, "V-BLAST: an architecture for realizing very high data rates over the rich-scattering wireless channel," *Proc. of International Symposium on Signals, Systems, and Electronics*, pp. 295-300, Sept. 29-Oct. 2, 1998.

- [26] D. Wubben, R. Bohnke, V. Kuhn and K.-D. Kammeyer, "MMSE extension of V-BLAST based on sorted QR decomposition," *Proc. of IEEE 58th Vehicular Technology Conference*, vol. 1, pp. 508–512, Oct. 6-9, 2003.
- [27] D. Wubben, R. Bohnke, V. Kuhn and K.-D. Kammeyer, "Near-maximum-likelihood detection of MIMO systems using MMSE-based lattice reduction," *Proc. of IEEE International Conf. on Communications*, vol. 2, pp. 798–802, Jun. 20-24, 2004.
- [28] Y. Xin, Z. Liu, and G. B. Giannakis, "High-rate layered space-time coding based on constellation precoding," *Proc. of Wireless Communications and Networking Conf.*, vol. 1, pp. 471-476, Orlando, FL, Mar. 17-21, 2002.
- [29] Y. Xin, Z. Wang and G. B. Giannakis, "Space-time diversity systems based on linear constellation precoding," *IEEE Trans. on Wireless Communications*, vol. 2, no. 2, pp. 294-309, Mar. 2003.
- [30] W. Zhang and X. Ma, "Performance analysis for V-BLAST systems with linear equalization," *Proc. of 39th Conf. on Information Sciences and Systems*, Johns Hopkins Univ., MD, Mar. 15-18, 2005.

APPENDICES

APPENDIX A: PROOF OF LEMMA 1

Suppose the joint probability density function (pdf) of X_n 's is $f(x_1, x_2, \dots, x_N)$.

The cumulative density function (cdf) of X_{min} is:

$$\begin{aligned} F(v) = P(x_{min} < v) &= 1 - P(x_{min} \geq v) \\ &= 1 - \int_v^\infty dx_1 \int_v^\infty dx_2 \cdots \int_v^\infty f(x_1, x_2, \dots, x_N) dx_N. \end{aligned} \quad (1)$$

Then, we can obtain the pdf of X_{min} by taking the derivative of the cdf:

$$\begin{aligned} f(v) = \frac{d}{dv} F(v) &= - \int_v^\infty dx_1 \frac{d}{dv} \left(\int_v^\infty dx_2 \cdots \int_v^\infty f(x_1, x_2, \dots, x_N) dx_N \right) \\ &\quad + \int_v^\infty dx_2 \cdots \int_v^\infty f(v, x_2, \dots, x_N) dx_N \\ &= \sum_{n=1}^N \int_v^\infty dx_1 \cdots \int_v^\infty dx_{n-1} \int_v^\infty dx_{n+1} \cdots \\ &\quad \int_v^\infty f(x_1, \dots, x_{n-1}, v, x_{n+1}, \dots, x_N) dx_N \\ &\leq \sum_{n=1}^N f_{X_n}(v), \end{aligned} \quad (2)$$

where $f_{X_n}(x)$ is the pdf of X_n . According to [9, p. 25], we know that for a central Chi-square random variable X_n with degrees of freedom $2M$, we have

$$P(x_n < \epsilon) = 1 - e^{-\epsilon/2} \sum_{k=0}^{M-1} \frac{\left(\frac{\epsilon}{2}\right)^k}{k!} = e^{-\epsilon/2} \sum_{k=M}^{\infty} \frac{\left(\frac{\epsilon}{2}\right)^k}{k!} \leq \left(\frac{\epsilon}{2}\right)^M = c_M \epsilon^M,$$

where $c_M := 2^{-M}$ is a constant only dependent on M . With this inequality, we can obtain:

$$P(x_{min} < \epsilon) = \int_0^\epsilon f(v)dv \leq \int_0^\epsilon \sum_{n=1}^N f_{X_n}(v)dv \leq \sum_{n=1}^N c_M \epsilon^M = c_u \epsilon^M, \quad (3)$$

where $c_u := Nc_M$. Thus, Lemma 1 is proved. We notice that, Lemma 1 can be generalized to X_n 's with other pdfs. ■

APPENDIX B: COMPLEX LLL ALGORITHM

Here, we give the details of complex LLL algorithm in conventional MATLAB notation in the following table.

INPUT: \mathbf{H}
OUTPUT: $\mathbf{Q}, \mathbf{R}, \mathbf{T}$
(1) $[\mathbf{Q}, \mathbf{R}] = \text{QR Decomposition}(\mathbf{H});$
(2) $\delta = 0.75;$
(3) $m = \text{size}(\mathbf{H}, 2);$
(4) $\mathbf{T} = \mathbf{I}_m;$
(5) $k = 2;$
(6) while $k \leq m$
(7) for $n = k - 1 : -1 : 1$
(8) $u = \text{round}((\mathbf{R}(n, k) / \mathbf{R}(n, n)));$
(9) if $u \sim 0$
(10) $\mathbf{R}(1 : n, k) = \mathbf{R}(1 : n, k) - u\mathbf{R}(1 : n, n);$
(11) $\mathbf{T}(:, k) = \mathbf{T}(:, k) - u\mathbf{T}(:, n);$
(12) end
(13) end
(14) if $\delta(\mathbf{R}(k-1, k-1)^2) > \ \mathbf{R}(k-1, k)^*\mathbf{Q}(:, k-1) + \mathbf{R}(k, k)^*\mathbf{Q}(:, k)\ ^2$
(15) Swap the (k-1) th and k th columns in \mathbf{R} and \mathbf{T}
(16) $\Theta = \begin{bmatrix} \alpha^* & \beta \\ -\beta & \alpha \end{bmatrix}$ where $\alpha = \frac{\mathbf{R}(k-1, k-1)}{\ \mathbf{R}(k-1:k, k-1)\ };$ $\beta = \frac{\mathbf{R}(k, k-1)}{\ \mathbf{R}(k-1:k, k-1)\ };$
(17) $\mathbf{R}(k-1 : k, k-1 : m) = \Theta\mathbf{R}(k-1 : k, k-1 : m);$
(18) $\mathbf{Q}(:, k-1 : k) = \mathbf{Q}(:, k-1 : k)\Theta^H;$
(19) $k = \max(k-1, 2);$
(20) else
(21) $k = k + 2;$
(22) end
(23) end

Table 1: The complex LLL algorithm

APPENDIX C: PROOF OF LEMMA 3

Let \mathbf{x} be a vector in the lattice \mathbf{L} . Since \mathbf{L} is spanned by the columns of \mathbf{H} , then \mathbf{x} can be expressed as $\mathbf{H}\mathbf{a}$, where \mathbf{a} is an $N \times 1$ column vector with all entries belonging to Gaussian integer ring. So based on the definition of \mathbf{h}_{min} , we can obtain:

$$\mathbf{h}_{min} = \arg \min_{\mathbf{x} \in \mathbf{L}, \mathbf{x} \neq \mathbf{0}} |\mathbf{x}|^2 = \mathbf{H}\mathbf{a}_H, \quad (4)$$

where $\mathbf{a}_H \in \mathbb{Z}[\sqrt{-1}]^{N \times 1}$. By defining an $MN \times 1$ vector $\mathbf{h} = [\mathbf{h}_1^T, \dots, \mathbf{h}_N^T]^T$, we have:

$$|\mathbf{h}_{min}|^2 = |\mathbf{H}\mathbf{a}_H|^2 = \mathbf{h}^{\mathcal{H}} (\mathbf{I}_M \otimes ((\mathbf{a}_H^T)^{\mathcal{H}} \mathbf{a}_H^T)) \mathbf{h} = \mathbf{h}^{\mathcal{H}} \mathbf{A}_H \mathbf{h}, \quad (5)$$

where $\mathbf{A}_H = \mathbf{I}_M \otimes ((\mathbf{a}_H^T)^{\mathcal{H}} \mathbf{a}_H^T)$. Suppose that the correlation matrix of the channel vector is $E[\mathbf{h}\mathbf{h}^{\mathcal{H}}] = \mathbf{R}_h$. The singular-value decomposition (SVD) of \mathbf{R}_h is $\mathbf{U}_h \mathbf{\Lambda}_h \mathbf{U}_h^{\mathcal{H}}$ where \mathbf{U}_h is a unitary matrix and $\mathbf{\Lambda}_h$ is a diagonal matrix with all singular values. Suppose $rank(\mathbf{R}_h) = R_h$ and define an $R_h \times 1$ vector $\tilde{\mathbf{h}}$ with i.i.d. entries. Then \mathbf{h} and $\mathbf{U}_h \mathbf{\Lambda}_h^{\frac{1}{2}} \tilde{\mathbf{h}}$ have identical distribution and thus the same statistical properties. Similar to pairwise error probability (PEP) analysis in [18] and [22], we can get an upper bound for the probability that $|\mathbf{h}_{min}|$ is less than ϵ by averaging (5) with respect to the random basis \mathbf{H} :

$$P(|\mathbf{h}_{min}|^2 \leq \epsilon) = P(\tilde{\mathbf{h}}^{\mathcal{H}} \mathbf{\Lambda}_h^{\frac{1}{2}} \mathbf{U}_h^{\mathcal{H}} \mathbf{A}_H \mathbf{U}_h \mathbf{\Lambda}_h^{\frac{1}{2}} \tilde{\mathbf{h}} \leq \epsilon) \leq c_h \epsilon^D, \quad (6)$$

where

$$D = \min_{\forall \mathbf{a}_H} \text{rank}(\mathbf{R}_h \mathbf{A}_H).$$

Since \mathbf{H} are complex Gaussian distributed, the set of possible \mathbf{a}_H can be the whole Gaussian integer ring. Thus, we can represent D as

$$D = \min_{\forall \mathbf{p} \neq \mathbf{0}} \text{rank}(E(\mathbf{p}\mathbf{p}^H)). \quad (7)$$

■

APPENDIX D: PROOF OF PROPOSITION 4

In (3.7), we have defined that $\mathbf{C} = (\mathbf{H}^{\mathcal{H}}\mathbf{H})^{-1}$. By properly permutating \mathbf{H} to $[\mathbf{h}_i, \mathbf{H}_i]$, where \mathbf{h}_i is the i th column of \mathbf{H} and \mathbf{H}_i denotes the rest columns, we obtain that

$$\mathbf{C} = (\mathbf{H}^{\mathcal{H}}\mathbf{H})^{-1} = \mathbf{P} \begin{bmatrix} \mathbf{h}_i^{\mathcal{H}}\mathbf{h}_i & \mathbf{h}_i^{\mathcal{H}}\mathbf{H}_i \\ \mathbf{H}_i^{\mathcal{H}}\mathbf{h}_i & \mathbf{H}_i^{\mathcal{H}}\mathbf{H}_i \end{bmatrix}^{-1} \mathbf{P}^T,$$

where \mathbf{P} is a permutation matrix such that $\mathbf{HP} = [\mathbf{h}_i \ \mathbf{H}_i]$. Based on the matrix inversion lemma, we know that the (i, i) th element of \mathbf{C} is

$$C_{ii} = \left(\mathbf{h}_i^{\mathcal{H}}\mathbf{h}_i - \mathbf{h}_i^{\mathcal{H}}\mathbf{H}_i (\mathbf{H}_i^{\mathcal{H}}\mathbf{H}_i)^{-1} \mathbf{H}_i^{\mathcal{H}}\mathbf{h}_i \right)^{-1}. \quad (8)$$

Suppose the singular value decomposition (SVD) of \mathbf{H}_i is $\mathbf{H}_i = \mathbf{VDU}^{\mathcal{H}}$, where \mathbf{V} is an $N_r \times (N_t - 1)$ unitary matrix, \mathbf{D} is an $(N_t - 1) \times (N_t - 1)$ diagonal matrix and \mathbf{U} is an $(N_t - 1) \times (N_t - 1)$ unitary matrix. Plugging this SVD result into (8), we are ready to verify that:

$$\mathbf{H}_i(\mathbf{H}_i^{\mathcal{H}}\mathbf{H}_i)^{-1}\mathbf{H}_i^{\mathcal{H}} = \mathbf{V}\mathbf{V}^{\mathcal{H}}.$$

It is straightforward to see that the rank of $\mathbf{V}\mathbf{V}^{\mathcal{H}}$ is $N_t - 1$. More specifically, $\mathbf{V}\mathbf{V}^{\mathcal{H}}$ is an $N_r \times N_r$ matrix whose eigenvalue decomposition can be written as:

$$\mathbf{V}\mathbf{V}^{\mathcal{H}} = \tilde{\mathbf{V}} \begin{bmatrix} \mathbf{I}_{N_t-1} & \mathbf{0}_{N_t-1, N_r-N_t+1} \\ \mathbf{0}_{N_r-N_t+1, N_t-1} & \mathbf{0}_{N_r-N_t+1, N_r-N_t+1} \end{bmatrix} \tilde{\mathbf{V}}^{\mathcal{H}},$$

where $\tilde{\mathbf{V}}$ is an $N_r \times N_r$ unitary matrix with the first $N_t - 1$ columns same as \mathbf{V} . This is because the matrix $\mathbf{V}\mathbf{V}^{\mathcal{H}}$ has the same non-zero eigenvalues as $\mathbf{V}^{\mathcal{H}}\mathbf{V}$. Therefore, we can verify

$$\begin{aligned} C_{ii}^{-1} &= \mathbf{h}_i^{\mathcal{H}}(\mathbf{I}_{N_r} - \mathbf{V}\mathbf{V}^{\mathcal{H}})\mathbf{h}_i \\ &= \mathbf{h}_i^{\mathcal{H}}\tilde{\mathbf{V}} \begin{bmatrix} \mathbf{0}_{N_t-1} & \mathbf{0}_{N_t-1, N_r-N_t+1} \\ \mathbf{0}_{N_r-N_t+1, N_t-1} & \mathbf{I}_{N_r-N_t+1, N_r-N_t+1} \end{bmatrix} \tilde{\mathbf{V}}^{\mathcal{H}}\mathbf{h}_i. \end{aligned}$$

It can be seen that the number of degrees of freedom in C_{ii}^{-1} is $2(N_r - N_t + 1)$. Furthermore, C_{ii}^{-1} is a chi-squared random variable with $2(N_r - N_t + 1)$ degrees of freedom, because the channel coefficients are complex Gaussian distributed. As shown in [22], if we integrate the right side of (2.7) with respect to this random variable, we obtain that the diversity order is equal to $N_r - N_t + 1$. This means the diversity order of the ZF detection is $N_r - N_t + 1$. ■